INVESTIGATION OF MXENES IN COMBINATIONAL PHOTOTHERMAL/PHOTODYNAMIC THERAPY AND IMMUNOTHERAPY

A THESIS SUBMITTED TO
THE GRADUATE SCHOOL OF NATURAL AND APPLIED SCIENCES
OF
ANKARA UNIVERSITY

by

Berfin İlayda ÖZTÜRK

DEPARTMENT OF BIOMEDICAL ENGINEERING

ANKARA
2024

All rights reserved

ABSTRACT

Master's Thesis

INVESTIGATION OF MXENES IN COMBINATIONAL PHOTOTHERMAL/PHOTODYNAMIC THERAPY AND IMMUNOTHERAPY

Berfin İlayda ÖZTÜRK

Ankara University
Graduate School of Natural and Applied Sciences
Department of Biomedical Engineering

Supervisor: Assoc. Prof. Açelya YILMAZER AKTUNA

Cancer is a leading global cause of mortality, resulting in millions of annual deaths. Novel cancer therapies are being developed in response to the elevated incidence of cancer and its associated mortality rates. Common conventional therapies encompass chemotherapy, radiotherapy, and surgery. Nevertheless, these techniques have significant adverse reactions on patients and the outcomes of the treatment are unsatisfactory. Novel approaches in cancer treatment encompass immunotherapy, gene therapy, photodynamic therapy (PDT), and photothermal therapy (PTT), which have enhanced or hold the potential to enhance therapeutic results. MXenes, which possess diverse physicochemical characteristics including a substantial surface area, notable electrical conductivity, magnetism, low toxicity, luminescence, and excellent biocompatibility, have been identified as highly promising contenders for cancer treatment. The 2D nanostructures possess photothermal, chemotherapeutic synergistic, and photodynamic properties, making them highly promising for efficient and non-invasive anticancer treatments. MXene, a 2D nanomaterial, has emerged as a viable substitute for traditional cancer therapy due to its photodynamic and photothermal characteristics. PTT and PDT are believed to induce immunogenic cell death (ICD) while also directly eliminating cancer cells. This thesis aims to conduct a comparative analysis of the photothermal/photodynamic therapeutic characteristics of MXene, a two-dimensional nanomaterial. Additionally, it examines whether MXene induces immunogenic cell death in vitro using the 4T1 cancer cell line, which serves as a representative model for human breast cancer.

March 2024, 76 pages

Key Words: Photothermal therapy, Photodynamic therapy, Immunotherapy, MXene

ÖZET

Yüksek Lisans Tezi

KOMBİNE FOTOTERMAL/FOTODİNAMIK TEDAVİ VE İMMÜNOTERAPİDE MXENLERIN ARAŞTIRILMASI

Berfin İlayda ÖZTÜRK

Ankara Üniversitesi
Fen Bilimleri Enstitüsü
Biyomedikal Mühendisliği Anabilim Dalı

Danışman: Doç. Dr. Açelya YILMAZER AKTUNA

Kanser, her yıl milyonlarca kişinin ölümüyle sonuçlanan, önde gelen küresel bir ölüm nedenidir. Artan kanser insidansı ve buna bağlı ölüm oranlarına yanıt olarak yeni kanser tedavileri geliştirilmektedir. Yaygın geleneksel tedaviler kemoterapi, radyoterapi ve cerrahiyi kapsamaktadır. Bununla birlikte, bu teknikler hastalar üzerinde önemli yan etkilere sahiptir ve tedavi sonuçları tatmin edici değildir. Kanser tedavisindeki yeni yaklaşımlar immünoterapi, gen terapisi, fotodinamik terapi (PDT) ve fototermal terapiyi (PTT) kapsamakta olup, bunlar terapötik sonuçları geliştirmiş veya geliştirme potansiyeline sahiptir. Önemli bir yüzey alanı, kayda değer elektrik iletkenliği, manyetizma, düşük toksisite, lüminesans ve mükemmel biyouyumluluk gibi çeşitli fizikokimyasal özelliklere sahip olan MXenler, kanser tedavisi için oldukça umut verici seçenekler olarak tanımlanmıştır. 2D nanoyapılar fototermal, kemoterapötik sinerjik ve fotodinamik özelliklere sahiptir ve bu da onları etkili ve non-invaziv antikanser tedavileri için oldukça umut verici kılmaktadır. Bir 2D nanomateryal olan MXene, fotodinamik ve fototermal özellikleri nedeniyle geleneksel kanser tedavisinin uygulanabilir bir alternatifi olarak ortaya çıkmıştır. FTT ve FDT'nin immünojenik hücre ölümünü (ICD) indüklerken aynı zamanda kanser hücrelerini doğrudan ortadan kaldırdığıda düşünülmektedir Bu tez çalışmasındada 2B nanomalzeme olan MXene'in Fototermal/Fotodinamik terapi özelliklerini karşılaştırmayı ve immünojenik hücre ölümünü tetikleyip tetiklemediği, insan meme kanserini yakından taklit eden 4T1 kanser hücre hattı ile in vitro olarak araştırılmıştır.

Mart 2024, 76 sayfa

Anahtar kelimeler: Fototermal Terapi, Fotodinamik terapi, İmmünoterapi, MXene

ACKNOWLEDGEMENTS

I am proud to complete my master's degree at Ankara University Biomedical Engineering Department where I have been studying since my undergraduate education and I would like to thank my esteemed professors and colleagues who shared their scientific knowledge with us.

I would like to express my endless thanks and respect to my supervisor, Assoc. Prof. Dr. Açelya YILMAZER AKTUNA, who shared her life experiences and invaluable knowledge and experiences throughout my undergraduate education and my master's thesis study.

I would like to thank the Scientific and Technical Research Council of Turkey for providing financial support for my thesis study within the scope of the 1004 project during my master's degree education, as well as Ankara University Biomedical Engineering Department, from whose materials and equipment I benefited during my thesis study.

I would like to thank Cansu Gürcan Karatepe, Esen Kirit, Cemile Gökçe, Hümeyra Hande Yavuz, Buse Altun and my other teammates who shared their valuable experiences with me and supported me throughout my thesis study. I would also like to thank Recep Uyara for his contributions to the bioinformatic analyses in my thesis.

I would like to thank Assoc. Prof. Dr. Ahmet CEYLAN, faculty member of Ankara University, Faculty of Veterinary Medicine, who contributed to obtaining TEM microscope and ultra-thin sections for my thesis study. I would like to thank Prof. Dr. Yury Gogotsi, member of A.J. Drexel Nanomaterials Institute, Department of Materials Science and Engineering, for the supply of MXene material used in my thesis study. I would also like to thank Prof. Dr. İbrahim Çağatay Karaaslan for sharing his knowledge and guidance on culturing CAL1 cells.

I would like to thank Fatma Kehya and Dağlar Akarsu Kaplana for their moral support and I would like to express my gratitude to Erdem Ezin and Çağlar Gürbüz for their friendship, guidance and support since my undergraduate studies.

I would like to thank my precious family for supporting me throughout my life; my mother Rabia ÖZTÜRK and my father Hasan ÖZTÜRK for their unconditional love and labour, and my precious sister Öykü Naz Öztürk. I would like to thank my dear Ozan GÜZELCAN, who patiently stood by me and supported me in good and bad times.

Berfin İlayda ÖZTÜRK
Ankara, March 2024

TABLE OF CONTENTS

THESIS APPROVAL
ETHICS....i
ABSTRACT....ii
ÖZET....iii
ACKNOWLEDGEMENTS....iv
TABLE OF CONTENTS....v
LIST OF SYMBOLS....vii
LIST OF FIGURES....viii
LIST OF TABLES....ix
1. INTRODUCTION....1
2. LITERATURE SURVEY....3
2.1 Cancer....3
2.2 Breast Cancer....4
2.3 Types of Cancer Treatments....6
2.3.1 Traditional types of cancer treatments....6
2.3.2 New procedures for cancer treatment....10
2.3.2.1 Cancer and stem cells....11
2.3.2.2 Targeted drug therapy....12
2.3.2.3 Gene therapy....13
2.3.2.4 Nanomedicine in cancer therapy....14
2.4 PDT&PTT....15
2.4.1 Photodynamic therapy (PDT)....16
2.4.2 Photothermal therapy (PTT)....18
2.5 Cancer Immunotherapy....20
2.6 2D Nanomaterials and MXenes....21
3. MATERIAL AND METHODS....28
3.1 Materials....28
3.2 Methods....28
3.2.1 Cell culture....29
3.2.1.1 Cell culture preparation....29
3.2.1.2 Passaging of cell lines and cell counting....30
3.2.1.3 Freezing and thawing cell lines....32

3.2.2 PTT and PDT protocol 35
3.2.3 LDH protocol 36
3.2.4 Optimization of proper mxene concentration and wavelength 37
3.2.5 Optimization of light duration 38
3.2.6 Temperature measurement experiment 39
3.2.7 Examination of ROS activity 39
3.2.8 TEM analysis 40
3.2.9 Statistical analysis 41
4. RESULTS 42
4.1 Determination of Appropriate Material Concentration and Wavelength 42
4.2 Determination of Light Exposure Time 45
4.3 Temperature Measurement Experiment 47
4.4 Examination of ROS Activity 48
4.5 TEM Analysis 51
5. DISCUSSION 60
6. CONCLUSION 64
REFERENCES 65
CURRICULUM VITAE 76

LIST OF SYMBOLS

°C	Degrees Celsius
nm	Nanometer
µg	Microgram
µl	Microliter

Abbreviations

PDT	Photodynamic Therapy
PTT	Photothermal Therapy
ICD	Immunogenic Cell Death
ROS	Reactive Oxygen Species
DNA	Deoxyribonucleic Acid
CSCs	Cancer Stem Cells
HSCs	Hematopoietic Stem Cells
BM	Bone Marrow
TME	Tumor Microenvironment
EVs	Extracellular Vesicles
EGFR	Epidermal Growth Factor Receptor
NSCLC	Non-Small Cell Lung Cancer
TIL	T-Cell Lymphocytes
PS	Photosensitizer
NIR	Near-Infrared
APCs	Antigen-Presenting Cells
GM-CSF	Granulocyte-Macrophage Colony-Stimulating Factor
PTCE	Photothermal Conversion Efficiency
PAI	Photoacoustic Imaging
Ta_4C_3	Tantalum Carbide
Nb_4C_3	Niobium carbide
$Mo_2Ti_2C_3$	Molybdenum
LDH	Lactate dehydrogenase
DMEM	Dulbecco's Modified Eagle Medium
FBS	Fetal Bovine Serum
Pen/Strep	Penicillin/Streptomycin
DPBS	Dulbecco′s Phosphate Buffered Saline
DMSO	Dimethylsulfoxide
TEM	Transmission Electron Microscopy

LIST OF FIGURES

Figure 2.1 Figure 2.1 Illustration of the PDT mechanism 17

Figure 2.2 Figure 2.2 Illustration of the PTT mechanism..... 19

Figure 3.1 Inverted light microscope image of 4T1 and CAL1 cell lines..... 34

Figure 3.2 Illustration of PTT&PDT protocol……35

Figure 3.3 4T1 cells exposed to LED light at wavelengths of 520 nm and 850 nm..... 38

Figure 4.1 Cell viability of 4T1 cells. Viability of cells treated with $Mo_2Ti_2C_3$ after PTT & PDT protocol……43

Figure 4.2 Cell viability of 4T1 cells. Viability of cells treated with Nb_4C_3 after PTT & PDT protocol……...…44

Figure 4.3 Cell viability of 4T1 cells. Viability of cells treated with Ta_4C_3 after PTT & PDT protocol. 45

Figure 4.4 4T1 cells were treated with $Mo_2Ti_2C_3$ at a concentration of 200 μg/ml for 4 hours followed by evaluation of cell viability in the presence of 850 nm led light for 0.5, 1 and 2 hours 46

Figure 4.5 The temperature rise following treatment of 4T1 cells with Mo2Ti2C3 at a concentration of 200 μg/ml for 4 hours was recorded using a non-contact temperature meter..... 48

Figure 4.6 Fluorescence microscope images of ROS activity after PTT&PDT protocol applied to 4T1 cells……...50

Figure 4.7 Schematic representation of PTT triggering ICD..... 52

Figure 4.8 TEM imaging of CAL1 cells 53

Figure 4.9 TEM imaging of endocytosis of material by CAL 54

Figure 4.10 TEM imaging of $Mo_2Ti_2C_3$ treated 4T1 cells show the material uptake via endocytic pathway ……..……55

Figure 4.11 TEM imaging of $Mo_2Ti_2C_3$ treated 4T1 cells show the material uptake via endocytic pathway ……...56

Figure 4.12 TEM imaging of phagocytosis of materials by CAL1 cells after PTT triggered immunotherapy 57

Figure 4.13 Material uptake of CAL1 cells after the PTT protocol..... 58

LIST OF TABLES

Table 2.1 FDA-Approved stem cell cancer therapies 12
Table 2.2 Combined cancer treatments with Mxenes 25
Table 3.1 Cell lines, passage numbers and cell medium content 29
Table 3.2 Mxene types and concentrations used in the optimization phase 37

1. INTRODUCTION

In 2019, the World Health Organization (WHO) underscored a sobering reality: cancer had become a leading cause of death, either primary or secondary, for individuals under the age of 70 in more than 110 countries. Furthermore, the incidence of new cancer cases and cancer-related fatalities is projected to rise in the coming years (Sung et al., 2021). The negative side effects of commonly used treatments and unsatisfactory treatment results have led to new searches for cancer treatment.

Photothermal therapy (PTT) is a recently developed technique used for cancer treatment. Objective of PTT is to eliminate cancer cells by transforming light into thermal energy (Cheng, Wang, Feng, Yang, & Liu, 2014). PTT stands as an intricate yet minimally invasive treatment approach, homing in on precise areas within the body. It operates by leveraging substances capable of absorbing energy and transforming it into heat upon exposure to specific forms of electromagnetic radiation. These radiation types encompass near-infrared irradiation, microwaves, radiofrequency,or visible radiation, orchestrating a targeted assault on the designated site (Eskiizmir, Baskın, & Yapıcı, 2018). During the course of treatment, a photosensitizer is stimulated by electromagnetic radiation, often in the near infrared range. The photosensitizer absorbs the energy and transforms it into heat, resulting in localized hyperthermia that enables extremely accurate tumor ablation (Ban, Bai, Duan, & Kong, 2017).

Photodynamic Therapy (PDT) presents a medical intervention employing both light and a photosensitizing agent to meticulously eradicate abnormal cells. This minimally invasive treatment modality capitalizes on tailored light wavelengths and a photosensitizer to induce reactive oxygen species (ROS) generation. Upon exposure to light, photosensitizers channel the absorbed photon energy to oxygen molecules, instigating the formation of free radicals (-O_2-) or singlet oxygen. Consequently, this cascade precipitates the demise of cancer cells while inflicting controlled damage to neighboring tissue (Aghajanzadeh et al., 2022).

Immunotherapy shows great potential in the therapeutic treatment of cancer, particularly for cases with recurring or metastasized cancer, which are recognized as challenging clinical situations. Research has been conducted on methods to boost the body's ability to fight diseases by improving the immune system's response, such as promoting cell death in the affected area and employing vaccines as a kind of treatment (K. Liu et al., 2022). Cancer immunotherapy depends on the effective display of tumor antigens to T-cells in order to provoke a strong immune response against the tumor and establish lasting immunological memory. This process leads to the destruction of cancer cells and prevents the return of cancer (Paulis, Mandal, Kreutz, & Figdor, 2013).

MXenes stand as compounds characterized by the formula $M_{n+1}X_nT_x$, wherein M signifies a transition metal (e.g., Mo, V, Cr and Ti), X denotes either nitrogen or carbon, n spans from 1 to 3, and Tx indicates surface functional groups for example -F and/or -O, -OH. These compounds emerge through a targeted extraction process, wherein the "A" layers predominantly composed of elements from groups 13 and 14 are selectively removed from layered ternary carbides termed MAX phases. This extraction is achieved utilizing agents for intance ammonium bifluoride (NH_4HF_2), hydrofluoric acid (HF), or a mixture of hydrochloric acid (HCl) and lithium fluoride (LiF) (Halim et al., 2016).In addition MXene is a highly efficient material because it has a wide surface area and can convert light into heat more effectively than traditional photothermal agents. Additionally, it facilitates precise infiltration of NIR light into the specific tissue, expedites the healing process, and minimizes the level of invasiveness. This enhances the utilization and prospective significance of MXene in the medicinal domain (Soleymaniha, Shahbazi, Rafieerad, Maleki, & Amiri, 2019).

This thesis endeavors to assess the photothermal and photodynamic impacts of MXene nanomaterial, alongside examining the survival rates of breast cancer cells under light exposure facilitated by the nanomaterial. Additionally, it aims to delve into the immunotherapeutic potential of combining PTT & PDT. For this reason, temperature increase and ROS analysis experiments were performed as a result of PTT/PDT protocols with the correct MXene concentration and TEM analyses were performed to determine whether the treatment method used triggers Immunogenic cell death (ICD).

2. LITERATURE SURVEY

2.1 Cancer

Cancer is distinguished by the unregulated proliferation of cells. Cancer cells have intricate and dynamic interactions with their surrounding environment, encompassing healthy neighboring cells as well as constituents of the immune system, which occur over a prolonged period of time (Reichert & Wenger, 2008).Cancer is widely recognized as a complex disease that arises from succession of sequential occurrences referred to as carcinogenesis, which involves the dysregulation of several cellular physiological mechanisms including cell signaling and apoptosis. Although cancer typically originates in a localized manner, it has the propensity to disseminate to distant anatomical locations (Zou, 2005).

The initiative known as the 'war on cancer', which was initiated during the 1970s, provided significant insights into the underlying biological mechanisms of cancer. However, it also unveiled the intricate nature of this issue (Cairns, 1985).Thus far, treatments for cancer have been administered based on clinical and pathologic staging, which is assessed by the use of morphologic diagnostic tools, including conventional radiographic and histological standardized testing. However, early diagnosis and definitive treatment of cancer is still a major problem today (Misra, Acharya, & Sahoo, 2010). Traditional approaches to cancer treatment often encounter numerous hurdles, including the indiscriminate distribution of anti-tumor medications throughout the body, inadequate drug concentrations reaching the targeted tumor site, concerns regarding cytotoxicity, restricted capabilities for monitoring treatment responses, and the development of multidrug resistance (Das, Mohanty, & Sahoo, 2009). Chemotherapy, radiation and surgery are among the most common treatments used today, but these treatment types do not offer an optimal treatment due to the disadvantages mentioned above (Cairns, 1985; Carr, Ng, & Wigmore, 2008; Chidambaram, Manavalan, & Kathiresan, 2011; Das et al., 2009; Gilman, 1963; Misra et al., 2010; Reichert & Wenger, 2008; Singhal, Nie, & Wang, 2010; Zou, 2005).

2.2 Breast Cancer

Among women, breast cancer stands out as the most prevalent form of cancer. Breast cancer also accounts for almost one third of all malignancies in women. When compared to other forms of cancer, breast cancer has the second highest morbidity rate after lung cancer (Richie & Swanson, 2003).

The symptoms and clinical signs of breast cancer are related to whether the disease has metastasized to surrounding tissues. Breast cancer often metastasises mainly to the lung, lymph nodes, skin, bones and central nervous system.When diagnosing breast cancer, the initial evaluation focuses on determining the disease's extent and the tumor's pathological characteristics. Following physical examination, imaging techniques are employed to gauge the spread of the disease. Pathological assessment involves evaluating tumor size, tumor grade, histological type, and the involvement of axillary lymph nodes (Frederick et al., 2002).

The clinical staging approach utilized for breast cancer serves as a method for characterizing the scope and intensity of the ailment, taking into account a range of aspects. The TNM method, which stands for Tumor, Node, and Metastasis, is commonly acknowledged as the primary staging system utilized for breast cancer.

a.Tumor (T): Primary tumor size and extent.

- **TX:** The assessment of the main tumor is inconclusive.
- **T0:** No primary tumor evidence found.
- **Tis:** Carcinoma in situ (non-invasive cancer).
- **T1, T2, T3, T4:** Growth of the original tumor. Higher numbers indicate bigger tumors or greater tissue invasion.

b. Node (N): It indicates if the malignancy has spread to surrounding lymph nodes.

- **NX:** The assessment of regional lymph nodes is not possible.
- **N0:** No evidence of regional lymph node involvement.

- **N1, N2, N3:** indicate a progressive escalation in the engagement of regional lymph nodes, with higher numerical values suggesting a greater extent of lymph node involvement.

c. Metastasis (M): This classification pertains to the presence or absence of metastasis, indicating the dissemination of cancer cells to far anatomical sites.

- **MX:** The assessment of distant metastases is not possible.
- **M0:** There is no evidence of distant metastases.
- **M1:** The presence of distant metastases is shown in M1.

- ✓ Stage 0 refers to the presence of carcinoma in situ, denoted as Tis, N0, M0. The neoplasm is localized inside the ducts or lobules and has not infiltrated adjacent tissues.
- ✓ Stage I refers to the early stage of a medical condition, characterized by the presence of a modest tumor size and the absence of any involvement of the lymph nodes.
- ✓ Phase II: Increased tumor dimensions or presence of adjacent lymph node infiltration.
- ✓ Stage III refers to a condition in which cancer has progressed to an advanced stage and is characterized by substantial involvement of lymph nodes.
- ✓ In Stage IV (Metastatic) cancer, the malignant cells have disseminated to remote regions of the body.

The inclusion of staging information plays a crucial role in informing therapy choices and offering a prognosis for the patient. It is noteworthy to acknowledge that the TNM system represents only a singular facet inside the whole evaluation of a patient afflicted with breast cancer. In addition to this system, additional variables, including hormone receptor status and HER2 status, are taken into account when formulating a treatment strategy. Furthermore, the progress made in comprehending the molecular attributes of breast

cancer is facilitating the development of treatment strategies that are tailored and focused on individual patients. It is advisable for patients to engage in a comprehensive dialogue with their healthcare team on their individual case and the available treatment alternatives (Thor, 2004).

2.3 Types of Cancer Treatments

2.3.1 Traditional types of cancer treatments

The therapy modalities and pharmacological interventions employed in the management of cancer are undergoing significant advancements due to the progress made in scientific research and technological innovations. Nevertheless, there exist certain conventional therapeutic approaches that have been employed for an extended period of time. The primary conventional therapeutic approaches can be enumerated as follows:

- ✓ Chemotherapy
- ✓ Surgical operation
- ✓ Radiotherapy

Chemotherapy: Chemotherapy can be succinctly characterized as a pharmacological intervention employing potent drugs to eradicate rapidly proliferating cells. The investigation of utilizing chemical agents for the treatment of cancer has a historical foundation spanning several centuries. However, it was during the 1940s that nitrogen mustards and antifolates were initially employed for the treatment of lymphoma in a patient. The present study can be characterized as the initiation of chemotherapy due to the detrimental impact of nitrogen mustard on the lymphatic system. However, it is noteworthy that despite an initial substantial antitumor response, the tumor quickly returned (Gilman, 1963).

The potent chemical agents employed to inhibit unregulated cellular proliferation and induce cell death exhibit the dual effect of eliminating malignant cells while concurrently

inflicting harm upon healthy cells. Furthermore, chemotherapy might give rise to adverse consequences, including but not limited to the occurrence of issues such as nausea, vomiting, and diarrhea in the affected individual (Carr et al., 2008).

Furthermore, the drawbacks of classical chemotherapy include the lack of selectivity of anticancer medications, limited water solubility, and the development of multidrug resistance (Chidambaram et al., 2011).

Surgical Operation : With the development of anaesthesia methods in 1846, surgery became a widely used medical intervention. The inception of medical imaging marked a significant milestone with the discovery of X-rays, subsequently paving the way for the introduction of radiography and CT scanning. These innovations enabled the precise localization and sizing of tumors, facilitating the utilization of surgery as a viable treatment option for cancer. Consequently, this progress propelled advancements in the field of oncological surgery (Thariat, Hannoun-Levi, Sun Myint, Vuong, & Gérard, 2013), (Peeters, Verbeeten Jr, & Venema, 1979).

Although surgery is a very important and frequently used method in cancer treatment, it has some disadvantages. For example, the tumour may have spread in inaccessible or very risky tissues. Or, due to the size and location of the tumour, surgery may result in the removal of functional tissues or organs, which may lead to loss of normal body functions. Furthermore, it should be noted that surgical intervention alone may not be deemed adequate in cases when the cancer has already undergone metastasis, thereby affecting distant organs or tissues. In such instances, a comprehensive treatment such as chemotherapy or targeted therapy may be required to address the proliferation of cancerous cells that have disseminated beyond the original tumor location (Lordick & Gockel, 2016),.

William Halstead's radical mastectomy technique, utilized in breast cancer surgery, showcased a local recurrence rate of 4%. Nonetheless, it is crucial to highlight that the long-term mortality rates due to cancer among his patients showed no significant alteration. While certain individuals were evidently cured solely through surgical

intervention, it was acknowledged that addressing local control as a result of pre-existing systemic metastatic dissemination constituted only a fraction of the complexities encountered in the treatment of other patients (Halsted, 1894).

Radiotherapy : Radiation is a form of physical energy that is employed in the eradication of cancerous cells. The type of radiation employed in this context is referred to as ionizing radiation due to its ability to generate ions, which are electrically charged particles, and transfer energy to the cells within the tissues it traverses. The energy that is deposited has the potential to induce cell death in cancer cells or instigate genetic alterations that ultimately lead to the demise of cancerous cells (Baskar, Lee, Yeo, & Yeoh, 2012).

High-energy radiation has the capacity to induce detrimental effects on the genetic material, specifically the deoxyribonucleic acid (DNA) within cells, hence impeding their capacity for cellular division and proliferation (Jackson & Bartek, 2009). Radiotherapy delivers high doses of radiation to the patient, killing cancerous cells, although not as much as chemotherapy, but also damaging healthy cells. However, normal cells have the ability to repair themselves faster than cancer cells and maintain normal function (Begg, Stewart, & Vens, 2011).

Despite being a widely utilized and efficacious approach in cancer treatment, radiation is accompanied by many drawbacks and prospective adverse effects: Firstly, akin to chemotherapy, this treatment modality might induce symptoms such as fatigue, cutaneous responses (manifesting as erythema, pruritus, and desquamation in the treated region), gastrointestinal distress including nausea, vomiting, and alterations in appetite. In addition to the aforementioned often observed side effects, there exist potential long-term hazards of cancer recurrence or metastasis. Furthermore, the impact of high-energy radiation on organ functions may vary depending on the specific tumor's location. In conclusion, it is worth noting that although radiotherapy is a commonly employed method for cancer treatment, prolonged exposure to radiation during this procedure may potentially elevate the likelihood of getting secondary malignancies over an extended period of time (Sourati, Ameri, & Malekzadeh, 2017).

Conventional therapeutics of breast cancer: Breast cancer prognosis varies depending on cancer type and timing of diagnosis. In instances where tumors have not metastasized, detection through mammography and general screening allows for localized treatment, minimizing the need for extensive interventions targeting other organs or tissues (Health, 1991).

Following surgical procedures for operable breast cancer, chemotherapy is frequently administered. However, for women with sizable operable tumors, preoperative chemotherapy offers potential advantages. Numerous studies have consistently demonstrated that approximately 90 percent of primary operable tumors experience a reduction in size exceeding 50 percent following chemotherapy. Consequently, this therapeutic intervention has rendered lumpectomy a viable alternative for a significant number of women who would have otherwise necessitated a mastectomy. When considering survival outcomes, there is no discernible benefit shown in relation to preoperative chemotherapy in comparison to postoperative chemotherapy (Fisher et al., 1997).

The most appropriate and favoured treatments for primary breast cancer use one or more modalities in combination. For example, systemic treatment with hormonal agents, combination chemotherapy or both. In locally treated breast cancer, chemotherapy, and hormone therapy in addition to treatment have a positive effect on the prognosis of the cancer. Additionally, there is a belief that combination chemotherapy, which entails the simultaneous application of multiple methods, proves to be more efficacious and lowers the annual risk of death by approximately 20 percent (Hortobagyi & Buzdar, 1995).

The clinical course of metastatic breast cancer displays significant variability, resulting in diverse rates of tumor progression and responses to systemic treatments. Management strategies for women with metastatic breast cancer typically involve some combination treatment. These are chemotherapy, hormone therapy, radiation, selective surgical interventions. Despite these efforts, it is important to acknowledge that prognosis for the majority of patients remains unfavorable, with a high likelihood of mortality from the disease. Consequently, the primary goals of treatment focus on providing appropriate

palliative care and extending life expectancy. This entails optimizing symptom control, mitigating adverse effects, and prolonging survival while minimizing disruptions to a woman's daily life and overall well-being through the comprehensive utilization of available therapeutic options (Greenberg et al., 1996), (Hortobagyi & Piccart-Gebhart, 1996).

Following the diagnosis of metastatic breast cancer, it is crucial to assess the spread and distribution of metastases. This evaluation guides the development of a comprehensive treatment plan, taking into account factors such as age, interval since disease-free status, hormone receptor status, and disease severity. Hormonal therapy emerges as the primary treatment option for women with limited and non-imminently life-threatening disease, especially those who are asymptomatic, elderly, or have estrogen receptor-positive tumors (Oncology, 1997).

Between 20% to 35% of women diagnosed with metastatic breast cancer experience a measurable and favorable response to initial hormone treatment. For those with receptor-positive tumors undergoing second-line hormonal therapy, the likelihood of achieving an objective response ranges from 10% to 20%. Moreover, an additional 15% to 30% of women may maintain stable disease status for at least six months or longer (Stuart et al., 1996),(Hortobagyi, 1998).

2.3.2 New procedures for cancer treatment

Cancer is a disease that starts with the loss of control over the proliferation of cells and the rate of progression varies (Sung et al., 2021). Historically, cancer patients had limited treatment options, predominantly relying on surgery, radiation therapy, chemotherapy, or a blend of these approaches for an extended period (Roy & Li, 2016). Recent advancements have led to a profound understanding of the intricate pathways underlying cancer progression and how they can be precisely targeted. This advancement is credited to the use of combinatorial techniques, which include the simultaneous use of numerous targeted therapies in combination with conventional chemotherapeutic agents like platinum compounds, taxanes. These combinations have demonstrated a synergistic

effect, surpassing the efficacy of individual therapies alone. For example, innovative approaches like pharmaceuticals, biological agents, and immune-based treatments are now employed in treating metastatic cancer, even in cases where the anticipated therapeutic outcome has not been attained. These methodologies are geared towards reducing mortality rates and prolonging survival durations.

2.3.2.1 Cancer and stem cells

Cancer stem cells (CSCs) arise from epigenetic mutations occurring in progenitor cells or normal stem cells. Their presence poses significant challenges in cancer treatment, primarily due to issues such as tumor growth, metastasis, and recurrence. Consequently, targeting CSCs holds promise in combating aggressive tumors (Chang, 2016).

Stem cells exhibit diverse mechanisms for tumor treatment. One such mechanism is homing, characterized by the swift migration of hematopoietic stem cells to specific stem cell niches within the bone marrow. Subsequently, transplants enter the engraftment phase, leading to the generation of specific blood cells Stem cells influence their surroundings through the secretion of paracrine factors, which encompass extracellular vesicles (EVs) and soluble substances. Furthermore, certain stem cell types, like transplanted hematopoietic stem cells (HSCs), possess the capacity to differentiate into various blood cell types, contributing to the production of a diverse array of blood cells (Vakhshiteh, Atyabi, & Ostad, 2019),(Reddy, 2005). Recent advancements in stem cell technologies offer considerable promise for tumor treatment. However, cancer stem cell therapy presents several notable side effects, including tumor recurrence, drug resistance, toxicity, autoimmune reactions, and susceptibility to viral infections (Chu et al., 2020).

Table 2.1 FDA-Approved stem cell cancer therapies

Types of Stem Cell	Cancer Type	Ref.
Adult Stem Cells	Ovarian Tumor	(Khalil et al., 2019)
Cancer Stem Cells	Acute Myelogenous Leukemia	(Konopleva et al., 2016)
Pluripotent Stem Cells	Prostate Cancer	(Ouyang, Telli, & Wu, 2019)

2.3.2.2 Targeted drug therapy

Targeted cancer therapies, often synonymous with terms like "molecularly targeted drugs," "molecularly targeted therapies," and "precision medicines," work by interfering with the activity of growth molecules. This disruption effectively hampers the proliferation and spread of cancer cells. The tumor microenvironment (TM), comprising various cellular components such as pericytes, smooth muscle cells, endothelial cells, fibroblasts, dendritic cells, inflammatory cells, and cancer stem cells, plays a crucial role in determining the origin and progression of a tumor(CSCs) (Aggarwal, 2010),(Adjei & Blanka, 2015).

Targeting cancer cells specifically with traditional chemotherapy is challenging due to their similarity to normal cells. Targeted pharmacological therapy agents engage various cellular mechanisms to combat these disorders, including halting the cell cycle, inducing apoptosis, preventing proliferation, and disrupting metabolic reprogramming (Valter et al., 2017). Enhancing treatment efficacy in cancer therapy can be pursued through two strategies: refining targeted therapies and directly targeting tumor cells for drug delivery (Bailey, Wojtkowiak, Hashim, & Gillies, 2012). Targeted therapy drugs employ distinct mechanisms compared to conventional chemotherapy drugs by selectively targeting cancer cells while minimizing harm to healthy cells, thereby distinguishing them from normal, healthy cells (Yadav, 2017).

Targeted cell agents can be categorized based on either their mode of action or their precise target site. Among these, some enzymes play a crucial role in stimulating the proliferation of cancer cells. Specific targeted medications work by inhibiting the activity of these enzymes, which act as signals for cancer cell growth. Known as enzyme inhibitors, these substances disrupt cellular signaling pathways, effectively impeding cancer growth and metastasis (Citri & Yarden, 2006). Certain targeted therapies are referred to be apoptosis-inducing medications due to their specific targeting of cellular components that regulate cell survival and death. These agents inhibit the formation of new blood vessels by tumors, hence aiding in the cessation of tumor growth by cutting off the blood flow to the tumors.

2.3.2.3 Gene therapy

Over the last two decades, notable advancements have occurred in cancer research and genomics. In 2001, two separate preliminary copies of the human genome sequence were published, along with the simultaneous discovery of some 30,000 genes (Lander, Linton, & Birren, 2001; Venter et al., 2001). As anticipated, this was then accompanied by thorough investigation in molecular genetics employing sophisticated instruments to analyze gene activity and investigate the biological mechanisms implicated in genetic abnormalities and the development of cancer (Dulbecco, 1986). The recent increase in understanding of cancer has resulted in the emergence of innovative methods for treating cancer, specifically gene therapy.

Gene therapy refers to any method aimed at treating or alleviating a condition by genetically changing a patient's cells (Strachan & Read, 1999). Over the years, novel methodologies have emerged to directly introduce genetic material (transgenes) into certain cells, with the goal of modifying their characteristics either temporarily or permanently. Target cells, ranging from normal cells to cancer cells, immune-mediated cells, or pluripotent stem cells, can be targeted by transgenic interventions. Transgenes, when inserted into cancer cells, may either trigger restore normal cellular activities or cell death. In normal cells, transgenes may either defend against drug-induced toxicity or stimulate immune cells to eliminate malignant cells. Molecular therapies for cancer,

utilizing gene- and vector-based approaches, encompass a wide range of methods aimed at modifying cancer cells, normal cells, and/or the tumor microenvironment (Weichselbaum & Kufe, 1997). For example, adoptive T-cell therapy has shown promise in inducing tumor regression in select individuals with solid tumors. In a recent investigation, researchers focused on patients with metastatic cervical cancer associated with human papillomavirus (HPV) who had shown resistance to chemotherapy and radiation treatment. These patients were selected based on their immune reactivity to HPV-E6 and HPV-E7. Tumor-infiltrating T-cell lymphocytes (TILs) were harvested from these patients and reintroduced into their bodies following a non-myeloablative conditioning regimen. Subsequently, patients received a high-dose of interleukin-2 (aldesleukin). Among the six patients exhibiting HPV reactivity, three showed objective tumor responses. Notably, two patients with metastatic disease achieved complete tumor regression for durations of 18 and 11 months post-treatment, with minimal occurrence of side effects (Hinrichs et al., 2014).

2.3.2.4 Nanomedicine in cancer therapy

The improved comprehension of the fundamental processes of tumor formation led to the identification and creation of highly targeted substances that can selectively influence certain proteins or pathways that are either overproduced or abnormal in tumors. The aim of targeting cell killing specificity was to mitigate the common adverse effects associated with conventional chemotherapeutic drugs, while concurrently achieving superior outcomes in terms of suppressing tumor growth. Notably, HER2, a subtype of human epidermal growth factor receptor 2, was found to be expressed in excess in 25 percent of breast cancer cases. This discovery prompted the creation of trastuzumab (Herceptin), a genetically engineered monoclonal antibody that attaches to the outer part of HER2 (Pegram, Konecny, & Slamon, 2000).

Nanotechnology has demonstrated the ability to overcome certain constraints associated with conventional chemotherapy to a certain degree, making it a useful asset for enhancing the overall effectiveness of cancer treatment. Typically, drug molecules are dissolved, adsorbed, entrapped, encapsulated, or bonded to nanomatrices. Nanocarriers,

with their small size (usually less than 500 nm) and high surface-area-to-volume ratios, can significantly impact the basic characteristics and biological effects of the substances they carry (Sung et al., 2021). In addition, nanoparticles can improve the absorption of medication that has low solubility in water, while also providing targeted delivery of the medication to tumors. Crucially, nanoformulations facilitate the selective accumulation of chemotherapeutic drugs in tumors, hence improving the effectiveness of treatment and minimizing damage in the rest of the body.

Currently, active targeting is widely used in cancer therapy as it enables drugs to accumulate primarily at tumor sites, while reducing their impact on healthy tissues. This approach enhances the effectiveness of treatment and reduces the risk of harmful side effects. As an illustration, liposomes used for medication targeting are frequently modified with different ligands or antibodies that specifically target tumors. These include folic acid, hyaluronic acid, antibodies, and aptamers. Liposomes and other nanocarriers can be designed using specialized materials to enable the controlled release of chemotherapeutics in response to the tumor microenvironment (TME). Nunes et al. conducted a recent work where they developed folate-conjugated pH-responsive liposomes to deliver irinotecan specifically to tumors. The formulation demonstrated a medication release profile that was based on the pH and showed improved uptake by the tumor cells. Remarkably, the liposomes that were dual-functionalized exhibited markedly superior effectiveness in combating colorectal cancer compared to the pH-sensitive system alone or the irinotecan that was not encapsulated (Nunes et al., 2021).

2.4 PDT&PTT

For over three thousand years, light therapy has served as a therapeutic method for addressing a diverse array of ailments (Daniell & Hill, 1991). For example, ancient civilizations such as the Egyptians, Indians, and Chinese employed light therapy as a therapeutic approach to address various conditions, including psoriasis, rickets, vitiligo, and skin cancer (Spikes, 1985). In the late 19th century in Denmark, Niels Finsen made groundbreaking strides in the use of light, known as 'phototherapy,' for disease treatment.

He found that exposing patients to red light could diminish the formation and discharge of smallpox pustules, rendering it an effective therapy for this ailment(Finsen, 1901).

2.4.1 Photodynamic therapy (PDT)

Photodynamic therapy (PDT) employs a photosensitizing medication and light to specifically harm the target tissue. Tissue damage also requires a sufficient quantity of molecular oxygen. In the absence of either of these components, there will be no impact, and so, achieving total efficacy requires meticulous planning of both medicine and light dosimetry. The medications are often administered systemically, however, the targeting mechanism primarily relies on the precise application of light, typically from a laser source, resulting in a localized impact rather than a systemic one (Brown, Brown, & Walker, 2004).

PDT involves combining two benign elements to produce cellular and tissue effects that rely on the presence of oxygen. The main element is the photosensitizer (PS), a light-sensitive chemical that may be accurately directed to certain cells or tissues. The second component entails a particular wavelength of light that activates the photosensitizer. When activated, the photosensitizer enables the conversion of light energy into molecular oxygen, leading to the generation of ROS. These reactions occur in close proximity to the photosensitizer, which absorbs the light. As a result, the photosensitizer selectively triggers biological responses in specific tissue regions exposed to light (Dolmans, Fukumura, & Jain, 2003). Photodynamic therapy (PDT) utilizes the energy emitted by light to eliminate malignant cells inside the specific tissue being treated. The photosensitizer takes energy from the light source and transfers it to molecular oxygen, resulting in the production of singlet oxygen, which is an energized version of oxygen. The singlet oxygen is the primary cytotoxic agent responsible for causing damage by swiftly interacting with biological components, eventually resulting in cell death and tumor removal (Gomer, Ferrario, & Fisher, 2001). PDT employs many strategies to eradicate tumors. A photosensitizer has the ability to specifically target tumor cells, causing either apoptosis or necrosis (Oleinick, Morris, & Belichenko, 2002). Alternatively, by specifically targeting the blood vessels of the tumor (or even the healthy

blood vessels around it), the tumor may be deprived of blood that carries oxygen. Therefore, by using PDT, the extent of tumor damage may be increased in conjunction with inflammatory and immunological reactions (Henderson & Dougherty, 1992).

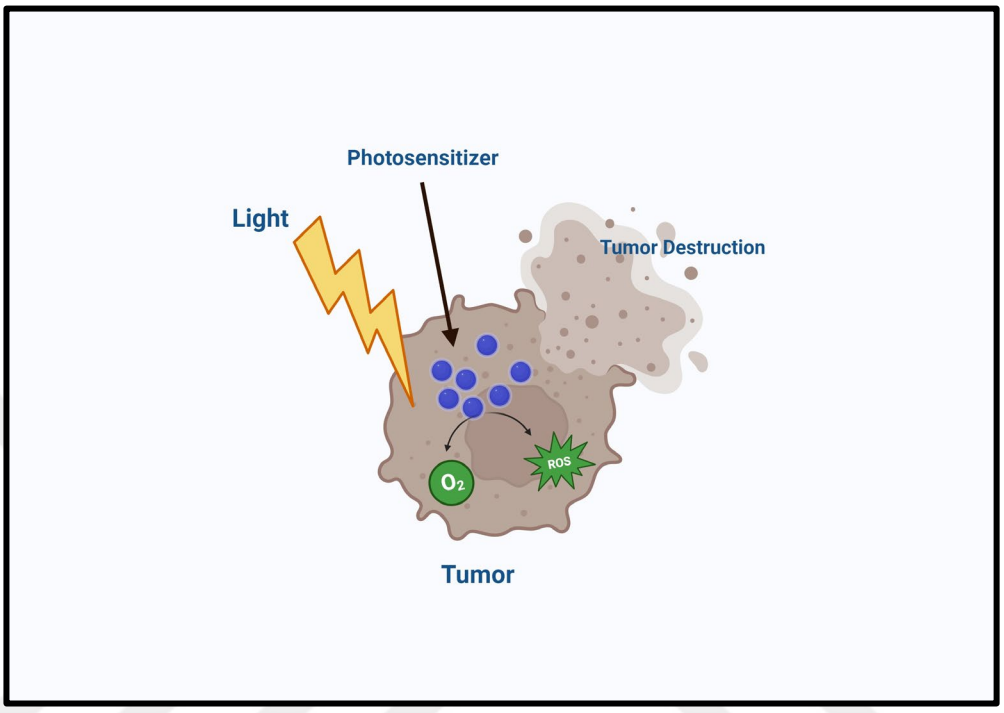

Figure 2.1 Illustration of the PDT mechanism

With the increasing use of nanomaterials in cancer research, the use of nanotechnology in PDT has become more interesting for reasons such as drug targeting, reducing toxicity, increasing drug solubility (Debele, Peng, & Tsai, 2015). Recent research have discovered many tumor-specific factors that might impede the effectiveness of photodynamic treatment for tumors. The formation of reactive oxygen species (ROS) mediated by PS is a mechanism that consumes oxygen. Nevertheless, the majority of solid tumors consistently experience a condition of low oxygen levels, known as hypoxia, which leads to different levels of resistance against photodynamic treatment. Furthermore, the excessive production of GSH in cancer cells may potentially mitigate the photodynamic harm caused by the resulting ROS(J.-n. Liu, Bu, & Shi, 2017)

2.4.2 Photothermal therapy (PTT)

Photothermal treatment (PTT) uses a near-infrared (NIR) laser via an optical fiber to treat tumors, whether they are on the surface or within the body. Light energy is absorbed and transformed into heat by optical absorption, causing the progressive ablation of the target tissue, either partly or completely, based on the PTT procedure. Utilizing selective photothermal absorbers and particular light wavelengths allows for precision targeting of difficult-to-treat cancers with little invasiveness. Moreover, advanced malignancies may be efficiently controlled by using partly destroyed tumors to trigger immune responses and introduce tumor antigens. The effectiveness of photothermal absorption in tumors depends on elements such the photothermal transducer, laser light wavelength, and the technique of light delivery. The main objective of laser light delivery systems in PTT is to evenly raise the temperature of tumor tissues while reducing harm to adjacent healthy tissues. Photothermal damage to tumor cells usually happens when the tumor temperature exceeds 41°C (Doughty et al., 2019). In addition, the temperature of the tumour centre is expected to be higher than 50 °C, since the tumour must not recur and the cancer cells must be destroyed (Hsiao et al., 2015),(C. Zhang et al., 2016).

Many different nanomaterials with different chemical structures can be used to increase light absorption in the target tissue. Recently, 2D nanomaterials have been frequently used as photothermal absorbers due to their unique chemical and electronic structures. PTT can be thought of as simply converting light of a certain wavelength into heat energy by means of a light absorber. Graphene oxide and Mxene are common examples of 2D nanomaterials with such light conversion capabilities. The illustration of PTT made using Mxene is shown in Figure 2.2.

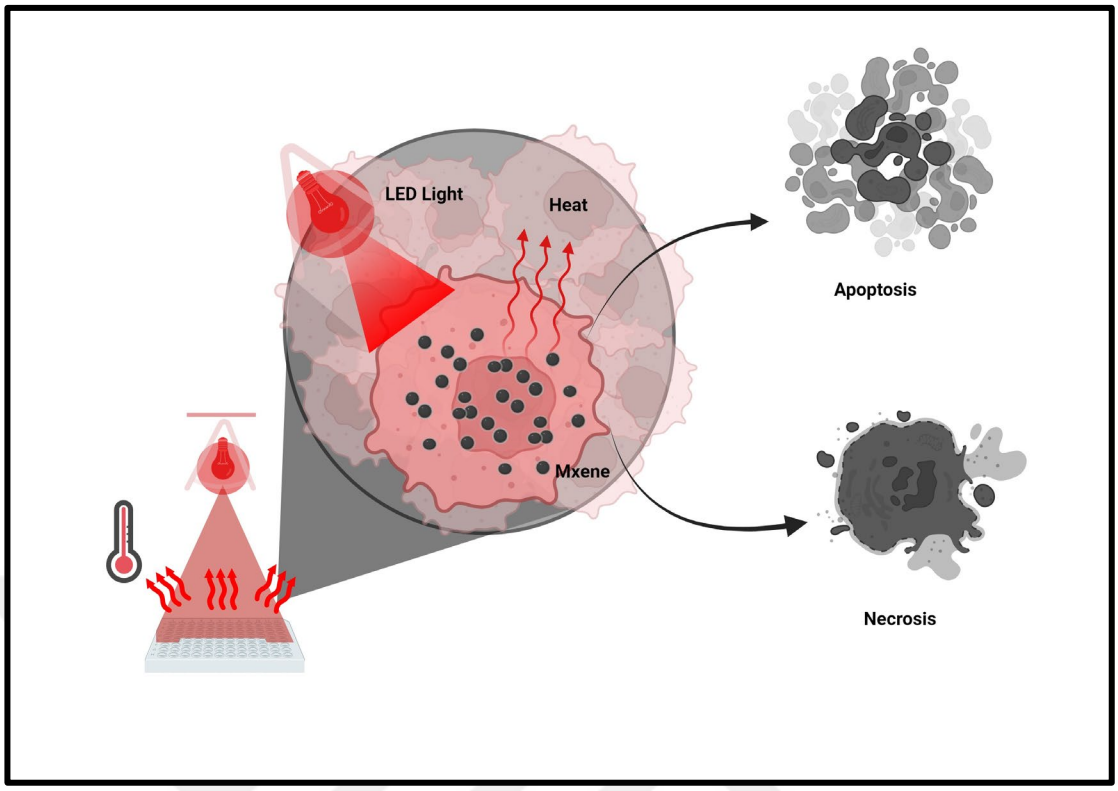

Figure 2.2 Illustration of the PTT mechanism

For example, in one study, Ma et al. created a composite structure conjugated with a phosphate scaffold using graphene oxide. In their in vivo experiments, they showcased the efficacy of their composite nanostructure in eradicating bone tumor cells through thermal ablation under near-infrared (NIR) light. Remarkably, over 80% of the tumor cells were observed to perish within 10 minutes of laser treatment (Ma et al., 2016). Graphene is another nanomaterial with a strong absorption capability in the wide NIR range in the newly emerging 2D MXenes. For instance, Lin et al. developed 2D biocompatible Ti_3C_2 nanosheets in a study. After 6 minutes of laser application, they confirmed by live-dead cell staining that the temperature rose rapidly to 55 °C and the 4T1 cells used in in vitro studies were destroyed. They also proved that the Ti_3C_2-SP nanosheets they created on the tumour model they created in mice have an effective tumour inhibition feature (H. Lin, Wang, Gao, Chen, & Shi, 2018).

2.5 Cancer Immunotherapy

Cancer immunotherapy involves harnessing and manipulating the immune system of body and its components to combat cancer effectively (Dillman, 2011). Cancer immunotherapy can be a good alternative or adjunctive treatment to existing cancer therapies because of its unique functions and effects in the face of all other treatments. Cancer immunotherapy has the ability to enable immune cells to selectively attack certain tumor cells while avoiding harm to healthy tissues, a capability that traditional therapies like surgery, radiation, and chemotherapy are unable to do. Illustrating this distinctive capability, cancer immunotherapy has the ability to selectively attack both the original tumor and any subsequent tumor metastases. Furthermore, during cancer immunotherapy, some immune cells have the ability to undergo differentiation into immunological memory cells. This results in a durable anti-tumor response and serves as a safeguard against tumor recurrence (Luo, Shu, & Wu, 2017). Cancer immunotherapy started with William Coley's use of bacterial toxins in 1890 (Kirkwood et al., 2008). Following additional advancements, in 2010, the FDA granted approval for the inaugural cellular immunotherapy of dendritic vaccine-based, trial known as sipuleucel-T, marking a significant milestone in the metastatic prostate cancer treatment (Palucka & Banchereau, 2012).

Antigen-presenting cells, notably dendritic cells serving as potent professional antigen-presenting cells, play a pivotal role in initiating the primary adaptive immune response in cancer immunotherapy,. After recognizing and internalizing protein antigens, immature DCs become activated and migrate to the lymph nodes. Within the lymph nodes, antigens are processed into peptides, which bind to major histocompatibility complex (MHC) molecules. The peptide-MHC complexes are displayed on the cell surface to be identified by naive T lymphocytes. Activated dendritic cells simultaneously release co-stimulatory chemicals to activate naive T cells. This mechanism encompasses two separate MHC pathways: MHC class II molecules presenting peptides from endosomes, identified by CD4 T cells, which then activate additional immune cells, and MHC class I molecules binding with peptides from the cytoplasm, detected by CD8 T cells. CD8 T cells can differentiate into cytotoxic T cells (CTLs), capable of directly eliminating tumor cells

(Luo et al., 2017). An important cytokine, granulocyte-macrophage colony-stimulating factor (GM-CSF), holds significant importance in immunotherapy due to its profound influence on the development and functionality of myeloid cells, notably monocytes, macrophages, and dendritic cells (Metcalf, 1985),(Gasson, 1991).

PTT is an innovative approach that utilizes specialized materials to convert absorbed optical radiation into heat, thereby destroying tumor cells. PTT and immunotherapy have been previously investigated in conjunction. For example Chen et al. aimed to address the challenges of eliminating primary tumors, inhibiting metastases, and preventing tumor relapse. They created a formulation using PLGA to contain both Indocyanine green (ICG) and imiquimod (R837) for a versatile treatment strategy. ICG acted like a photothermal agent in this approach, successfully destroying the main tumor when exposed to near-infrared laser light. Simultaneously, adding adjuvant R837 helped release tumor-associated antigens, giving the substance vaccine-like characteristics. This triggered a strong immunological reaction, especially powerful when used in conjunction with anti-cytotoxic T-lymphocyte antigen-4 checkpoint-blockade treatment. These components work together to enhance the treatment's effectiveness by focusing on primary tumors, preventing metastases, and reducing the chances of tumor recurrence (Q. Chen et al., 2016).

2.6 2D Nanomaterials and MXenes

The meticulous examination of the diverse dynamics and heterogeneous characteristics of cancer has led to a noteworthy focus on a novel category termed "nano-biomedicine." This interdisciplinary approach integrates imaging diagnostic techniques with potent therapeutic drugs designed for effective tumor removal. Nano-biomedicine encompasses the utilization of nanomaterials in the realm of biomedicine, specifically for the diagnosis and treatment of diseases. In recent times, the integration of various nanomaterials with biological therapies has gained prominence. Notably, 2D nanomaterials have emerged as standout contributors to the diagnosis and treatment of cancer, establishing themselves as highly valuable materials in the expansive landscape of nanomedicine applications (Yongjiu Chen, Wu, Sun, Liu, & Liu, 2017),(Naguib et al., 2011).

The fascination with 2D nanomaterials stems from their distinctive attributes, including few-layer nanostructures, expansive lateral planar configurations, and unparalleled physical and chemical properties. Recent years have witnessed a surge in research exploring diverse 2D nanomaterial systems for applications in biomedicine. The expansive surface area, distinctive surface chemical functionalities, and inherent optical characteristics render these materials well-suited for a myriad of roles in the field of nanobiomedicine.

Graphene, a single sheet of graphite, was originally discovered by Geim and colleagues in 2004, and has since generated considerable interest for the investigation of two-dimensional nanomaterials (2DNMs). 2DNMs are ultrathin nanomaterials that have a dimension smaller than 100 nm. Because of its exclusive structure, 2-dimensional nanomaterials (2DNMs) possess exceptional mechanical, thermal, optical, and chemical, properties. These advantageous traits have spurred significant research endeavors aimed at leveraging 2DNMs in various applications like energy storage, energy transport, and electrical also mechanical systems (Cheng, Wang, Gong, Liu, & Liu, 2020). Several research teams have developed tumor-targeted graphene oxide nanosheets for photothermal therapy, aiming to improve therapeutic specificity and attain precise tumor localization. In one study, Dai and colleagues utilized non-covalently PEGylated nano-rGO in conjunction with the targeting peptide Arg-Gly Asp to selectively induce photothermal destruction of U87MG cancer cells (Robinson et al., 2011).

A research by Akhavan et al. shown that a very low concentration of PEGylated GO nanoribbons modified with Arg-Gly Asp peptide might be used to localized photothermal therapy (Akhavan & Ghaderi, 2013). Additionally, the researchers generated a potent in vivo photothermal agent by employing RGD-functionalized rGO nanomeshes in a mouse model (Akhavan, Ghaderi, Aghayee, Fereydooni, & Talebi, 2012). The GO nanomeshes underwent modification with PEG, RGD, and Cy7 for targeting cancer in vivo and for fluorescence imaging of tumors in mice. When subjected to 808 nm irradiation, the rGO nanomesh-PEG solution exhibited approximately 5 times greater near-infrared (NIR) absorption compared to rGO-PEG and approximately 22 times higher absorption than pure GO (Liao et al., 2010).

AuNPs-mediated photothermal treatment (PTT) is increasingly utilized in both laboratory research and medical fields. Its advantages in cancer therapy surpass traditional thermal ablation due to its adaptable irradiation light and ability to induce internal hyperthermia. A variety of AuNPs with different sizes and structures, including nanospheres, nanocages, nanoshells, and nanorods, can be synthesized for this purpose (Hwang et al., 2014). AuNPs of different shapes possess distinct characteristics that might be used in various photothermal therapy methods for cancer treatment. AuNPs may absorb light and quickly transform it into heat, causing little injury to surrounding tissues. Manipulating the size, shape, spacing of particles, nanoparticle surroundings, and dielectric properties may modify the intensity and optical features (Ahmad, Fu, He, & Li, 2016). Hirsch et al. studied breast cancer cells exposed to an 820-nm near-infrared laser. Cells exposed to high doses of NIR laser without NPs were shown to stay alive. Cells cultured with nanoparticles without laser exposure remained viable, suggesting that neither treatment is independently damaging. Combining the two treatments led to specific cell death in the laser/NPs treatment region (Hirsch et al., 2003).

In 2011, Naguib, Gogotsi, and colleagues at Drexel University uncovered the first member of the MXene family: 2D Ti_3C_2 powder, composed of Titanium carbide (Naguib, Mochalin, Barsoum, & Gogotsi, 2014). MXenes, with their distinctive structural and electronic properties, stand out as one of the earliest types of two-dimensional materials employed in a multitude of applications (Sobolčiak, Tanvir, Sadasivuni, & Krupa, 2019). Belonging to the class of chemically etched metal carbonitrides and carbides, these materials are characterized by a general formula $M_{n+1}X_nT_x$. The symbol M represents elements like Mn, Ti, Nb, Cr, V, Hf, Zr, Sc, Wd, among others, while N or C may also be present, with n typically ranging from one to two.

MXene exhibits photothermal efficacy, enabling the conversion of laser light energy into heat by enhancing surface plasmon efficiency. Furthermore, its remarkable high photothermal conversion efficiency (PTCE) allows for substantial heat generation when exposed to laser irradiation. Leveraging these distinctive qualities, MXene materials have been tailored for diverse biomedical uses, such as drug delivery nanoplatforms, in vivo photoacoustic imaging (PAI), PTT (Lu et al., 2021). Consequently, researchers have

explored the application of MXenes in the context of PTT for cancer treatment. This involves leveraging MXenes to induce elevated temperatures, leading to the denaturation of proteins and, ultimately, the demise of cancer cells, contributing to the targeted eradication of tumors (G. Liu et al., 2017),(X. Wang & Cheng, 2019). For instance, Tantalum carbide (Ta_4C_3), classified as a MXene material, boasts a high photothermal conversion efficiency (PTCE), making it a viable candidate for cancer PTT. Lin et al. innovatively crafted MXene biomaterials with dual-mode photoacoustic/CT imaging capabilities and PTT functionality at an atomic thickness within the body. These biomaterials, derived from the exfoliation of MXene into ultrathin nanosheets, demonstrated outstanding PTCE performance at 44.7% and showcased in vitro/in vivo photothermal ablation using biocompatible soybean. Given the extensive MXene family, this investigation offers foundational research findings, suggesting the potential of MXene for specific biomedical applications (Zong, Wu, Lin, & Chen, 2018a). The another addition to the MXene family, Niobium carbide (Nb_2C), stands out for its exceptionally high photothermal conversion efficiency (PTCE). In their research, Lin et al. employed a combination of traditional HF etching, TPAOH intercalation, and a liquid phase stripping method to fabricate a monolayer of Nb_2C –MXene. To enhance biocompatibility and stability in physiological environments, the resulting nanosheets were modified with PVP (polyvinylpyrrolidone). When evaluating the photothermal conversion efficiency (PTCE) across different near-infrared (NIR) light ranges—specifically, NIR-I (808 nm) and NIR-II (1064 nm)—the researchers noted wavelength-dependent PTCE values: 36.4% at 808 nm and 45.65% at 1064 nm. Since the deeper tissue penetration of longer-wavelength NIR light, Nb_2C–PVP nanosheets exhibited effective in vivo photothermal ablation of tumor xenografts under both NIR-I and NIR-II. This highlights promising potential of Nb_2C–MXene in long-wavelength photothermal therapy, enabling applications like photoacoustic imaging (PAI) also PTT in deeply embedded tissues (H. Lin, Gao, Dai, Chen, & Shi, 2017). Apart from these examples, MXenes have been used in many PTT and combined cancer treatment studies (Table2).

Currently, immunotherapy is increasingly gaining attention. The therapy aims to activate or educate the patient's immune system to combat tumor cells, particularly those that have spread to other parts of the body (Jinbin Pan et al., 2018).Immunotherapy in conjunction

with photothermal PTT may enhance cancer treatment efficacy and reduce the likelihood of recurrence. Vaccination against cancer is successful in stimulating antitumor immune response. Most spherical or rod-shaped PTAs have a restricted capacity for loading antigens or adjuvants (Yu Chen, Wang, & Shi, 2016). 2D nanomaterials with enhanced specific surface areas have the potential to serve as efficient carriers or adjuvants for stimulating immune responses. Qu and collaborators developed a complex (GO-PEG-PEI-CpG) by covalently linking graphene oxide (GO) to polyethyleneimine (PEI) and polyethylene glycol (PEG), aiming to deliver unmethylated cytosine-phosphate-guanine (CpG) for photothermal-immunotherapy. The combination led to higher secretion levels of TNF-α and interleukin-6 compared to CpG alone, suggesting that GO-PEG-PEI might improve the absorption efficiency of CpG adjuvant. Furthermore, hyperthermia induced by the treatment could enhance cell membrane permeability, facilitating the endocytosis of GO-PEG-PEI-CpG and resulting in increased cytokine production levels compared to samples without irradiation (Tao, Ju, Ren, & Qu, 2014).Furthermore Han et al. used PEG-modified MoS_2 to encapsulate CpG, creating MoS_2-PEG-CpG. MoS_2 nanosheets had a greater CpG loading rate of 25% compared to graphene. MoS_2-PEG-CpG, when exposed to NIR light, efficiently induces dendritic cell maturation (Q. Han et al., 2017).

Table 2.2 Combined cancer treatments with Mxenes

Material	Application	Laser Wavelength (nm)	Ref
Ti_3AlC_2QD	PTT	808	(Yu et al., 2017)
T_3C_2@Au	PTT +Radiotherapy	1064	(W. Tang et al., 2018)
Ti_2C _PEG	PTT	808	(Szuplewska et al., 2019)
Nb_2C	PTT	808/1064	(H. Lin, Gao, et al., 2017)
MnO_x/Ta_4C_3−SP	PTT	808	(Dai, Chen, et al., 2017)
Ti_3C_2+DOX	PTT+ Chemotherapy	808	(X. Han, Huang, et al., 2018)
(Ti_3C_2)-Integrated Cellulose Hydrogels+DOX	PTT+ Chemotherapy	808	(Xing et al., 2018)
Ti_3C_2+DOX-HA	PTT + PDT+Chemotherapy	808	(G. Liu et al., 2017)

Table 2.2 Combined cancer treatments with Mxenes (continue)

MnO_x/Ti_3C_2	PTT	808	(Dai, Lin, et al., 2017)
Ta_4C_3-Fe_3O_4	PTT+ Chemotherapy	808	(Z. Liu, Lin, et al., 2018)
$MnFe_2O_4$@TiC_2-Chitosan	PTT	808	(Wu et al., 2022)
PVP/MnO_2-Ti_3C_2	PTT+ Chemotherapy	808	(J. Li et al., 2022)
GdW_{10}@Ti_3C_2	PTT	808	(Zong, Wu, Lin, & Chen, 2018b)
Ti_2N QDs	PTT	808/1064	(Shao, Zhang, Jiang, Lin, & Huang, 2020)
UCNPs@Ti_3C_2Tx	PDT+ Immunotherapy	655, 808, 980 and 1064	(D. Xu et al., 2020)
Ti_3C_2@IR780	PTT	808	(Y. Lin et al., 2022)
Ti_3C_2-CoNWs+DOX	PTT+ Chemotherapy	808	(Y. Liu et al., 2020)
CTAC@Nb_2C-MSN-PEG-RGD	PTT+ Chemotherapy	808/1064	(X. Han, Jing, et al., 2018)
Ti_3C_2-PVP@DOXjade	PTT+ Chemotherapy	808	(Y. Xu et al., 2022)
Ti_3C_2-GOX-CPO/TPZ	PTT+ Enzyme Dynamic Therapy +Hypoxia-Activated Chemotherapy	808	(X. Zhang et al., 2022)
Ta_4AlC_3	PTT	808	(H. Lin et al., 2018)
DOX+Ti_3C_2@mMSNs-RGD	Chemotherapy +PTT	808	(Z. Li et al., 2018)
Ti_3C_2−SP	PTT	808	(H. Lin, Wang, Yu, Chen, & Shi, 2017)
Ti_3C_2–IONPs–SPs	PTT	808	(Z. Liu, Zhao, et al., 2018)
Ti_3C_2@TiO_2-x-PEG	Sonodynamic therapy +PTT	1064	(D.-Y. Zhang et al., 2022)
TUT NPs (@Ti_3AlC_2)	PTT+ PDT	808	(Y. Wang et al., 2022)
$NaErF_4$@Ti_3C_2	PTT	808	(Jialin Pan et al., 2022)
$W_{1.33}C$-BSA	PTT	808, 1064	(B. Zhou et al., 2021)
MXene@Au-PEG-DO	Chemotherapy +PTT	808	(A. Liu et al., 2022)
$Ti_3C_2T_x$	PTT	1064	(Kyrylenko et al., 2022)

Table 2.2 Combined cancer treatments with Mxenes (continue)

$T3AlC_2$ terminated with $Al(OH)_4$	PTT	808	(Xuan et al., 2016)
Ti_3C2Tx @gelatin hydrogel	PTT	808	(You et al., 2021)
Ti_3C_2 MXene nanosheets	PDT+PTT	808 and 671	(Korupalli et al., 2022)
Mo_2C	PTT	1064	(Q. Zhang et al., 2019)

3. MATERIAL AND METHODS

3.1 Materials

CELL CULTURES		
DMEM (Dulbecco's Modified Eagle Medium)	Gibco™	4T1 Cells Expansion Medium
RPMI-1640 (1x)	Gibco™	CAL1 Cells Expansion Medium
FBS (Fetal Bovine Serum)	Gibco™	4T1-CAL1 Cells Expansion Medium
Penicillin/Streptomycin (Pen/Strep)	Biological Industries	4T1-CAL1 Cells Expansion Medium
L-Glutamine (100x)	Gibco™	CAL1 Cells Expansion Medium
Trypsin-EDTA(1X)	Gibco™	4T1-CAL1 Cell Passaging
DPBS (Dulbecco′s Phosphate Buffered Saline)	Gibco™	4T1-CAL1 Cell Passaging
ASSAYS		
CyQuant™ LDH Cytotoxicity Assay	Thermo Fisher Scientific	Cell viability analysis
DCFDA Cellular ROS Detection Assay Kit, ab113851	ABCAM	Examination of ROS Activity
GM-CSF (Granulocyte-macrophage colony-stimulating factor)	Thermo Fisher Scientific	TEM Analysis
Glutaraldehyde	Sigma-Aldrich	TEM Analysis

3.2 Methods

The material selection and cell culture studies of this thesis were carried out in the laboratories of Ankara University, Department of Biomedical Engineering. TEM images for this thesis study were acquired at Ankara University, Faculty of Veterinary Medicine Laboratories, under the supervision of Dr. Ahmet Ceylan. The $Mo_2Ti_2C_3$ material utilized in this research was generously supplied by Yury Gogotsi, a distinguished professor of materials science and Trustee Chair at Drexel University.

3.2.1 Cell culture

3.2.1.1 Cell culture preparation

This thesis study utilized the 4T1 cancer cell line, which closely emulates human breast cancer, as well as the CAL-1 cell lines, which represent human plasmacytoid dendritic cells. Table 3.2 provides comprehensive details regarding the passage number and culture media information for these two cell lines.

Table 3.1 Cell lines, passage numbers and cell medium content

Passage Numbers	Cell Lines	Cell Names	Medium Content
+3	4T1	Mouse Breast Cancer Cells	Hdmem + %10 Fbs + % 1 Pen/Strep
+5	CAL1	Human Plasmacytoid Dendritic Cells	Rpmı + %10 Fbs + % 1 Pen/Strep + % 1 L Glutamin

This thesis study utilized the 4T1 breast cancer cell line, which closely resembles human breast cancer, and the CAL-1 Human plasmacytoid dendritic cell lines to evaluate the immunogenic activity of the material and therapy. The cell lines were cultured using a laminar class II cabinet equipped with ultraviolet light sterilization. The preparation of DMEM medium for the 4T1 cell line involved the addition of 1% Pen/Strep and 10% FBS. The medium for CAL1 cells was produced by adding 1% penicillin streptomycin, 10% FBS, and 1% L Glutamine to RPMI 1640 Medium.

3.2.1.2 Passaging of cell lines and cell counting

Cells were passaged to maintain the uninterrupted growth of cultivated cells and eliminate metabolic byproducts. Cell counting was conducted to ascertain the appropriate cell densities for the research.

For the 4T1 cell line,

- The culture dishes that were taken out of the incubator were aspirated in order to eliminate the previous media.
- The flasks were rinsed with 3-5 millilitres (ml) of Dulbecco's Phosphate Buffered Saline (DPBS) in order to eliminate serum and metabolic waste from the medium. The DPBS in the flask was removed by aspiration to eliminate deceased cells from the culture.
- Subsequently, a volume of 1.5 ml of trypsin-EDTA was used to fully cover the surface of the flask, and the cells were incubated for a duration of 3-5 minutes.
- Following the designated period of waiting, the cells that had attached to the culture dish with the assistance of trypsin were detached from the culture dish. Next, the culture dish taken out of the incubator was lightly tapped to avoid cell adhesion and the formation of cell clusters on the flask's surface. The culture dish was then seen using an inverted light microscope.
- The flask was supplemented with three times the quantity of trypsin supplied, and the cells were evenly dispersed in the media with gentle pipetting. Based on the cell density, a specific volume of cell suspension was retained in the culture dish while the remainder cell suspension was disposed of. The medium was introduced into the cell suspension remaining in the culture vessel at a specific rate based on the size of the flask, and subsequently, the flask was transferred to the incubator.

For the CAL1 cell line,

- Since the CAL1 cell line is suspended, the cells in the flask are transferred directly into the falcon tube.

- The cells transferred to the vial tube are saturated at 800 rpm for 5 min and the cells are collected at the bottom. Then the supernatant is removed from the pellet as much as possible.
- The cells at the bottom of the flask are tapped with light blows to remove the cells at the bottom and fresh medium is added. By pipetting gently, homogenous distribution of the cells in the medium was ensured.
- Depending on the cell density, a certain volume of cell suspension was transferred to the culture dish and the remaining cell suspension was discarded. Depending on the size of the flask, a certain amount of medium was added to the cell suspension remaining in the culture dish and then the flask was transferred to the incubator.

For Cell Counting,

- Cells are harvested from either the cell line by using trypsin or directly from the flasks and transferred into falcon tubes.
- The gathered cells are thereafter subjected to centrifugation at a speed of 800 revolutions per minute for a duration of 5 minutes. The supernatant is discarded without touching the pellet and the pellet is dissolved by gently tapping the falcon tube.
- The Falkon tube was supplemented with 5-8 ml of media based on the specified cell density. In order to achieve a uniform distribution of cells in the media, the falcon tube was gently agitated laterally.
- A volume of 10 µl of the cell suspension was extracted and deposited onto the haemocytometer slide for the purpose of quantifying the cells. The quantification process was carried out using an inverted light microscope.

There are four large square areas in the field of hemositometry, and each square has an area of 1 mm2. The thickness of the gap between the hemositometer and the cover slip is 0.1 mm. Thus, the volume of each large square on the surface of the lamina is 0.1 mm^3. After adding the cell solution to the hemositometer slide, the cells in these four large squares are counted and their average is calculated. The standard method is used to calculate the number of cells in a volume of 0.1 mm^3 in milliliters (1 ml = 1 cm^3 = 1000

mm3). The average cell count is multiplied by 10,000 to calculate the number of cells in 1ml.

3.2.1.3 Freezing and thawing cell lines

The cultured cell lines were frozen, backed up and stored for repetition of experiments and for further experiments and studies. A unique cryopreservation solution was formulated for the purpose of cell freezing. The freezing solution consisted of FBS and DMSO in a 9:1 ratio, with 90% FBS and 10% DMSO (dimethylsulfoxide).

- The cells in the flasks were transferred either immediately to falcon tubes with trypsin or straight from the flasks, depending on the kind of cell line, as previously explained. The cells were then centrifuged at a speed of 11,000 revolutions per minute for a duration of 5 minutes.
- Following centrifugation, the supernatant was carefully removed, and the pellet was thawed by gently tapping the Falcon tube.
- The thawed pellet was supplemented with freezing medium, taking into account the cell density. The cells in the freezing solution were uniformly distributed by pipetting to guarantee homogeneity.
- The cell suspension was aliquoted into 1 ml freezing tubes, with relevant information such as the date and number of passages recorded on each tube. The tubes were then placed in a Mr. Frosty container and stored at a temperature of -80°C.
- After a day, the tubes were taken out from a temperature of -80°C and transferred to a nitrogen tank with a temperature of -196°C.

Frozen cells can be thawed and reused for repeating experiments or for new experiments.

- The cells in freezing tubes in nitrogen tank were kept in a water bath heated to 37°C for 30 seconds to 1 minute until a piece of ice remained in the tube.

- Then 2 ml of fresh media of the cell line was drawn into the serological pipette and the cells in the freezing tube were collected into the same serological pipette and transferred to the phalanx and the volume was filled with 5 ml of fresh media.
- The flask is centrifuged at 260 g for 5 minute and the supernatant is aspirated.Gently dıstrıbute the pellet by gently tappıng the pellet and gently pıpetage by addıng the requıred amount of medıum and transfer the cells to the flask then ınsert the flasks ın the ıncubator at 37 °c and 5% CO_2 density.

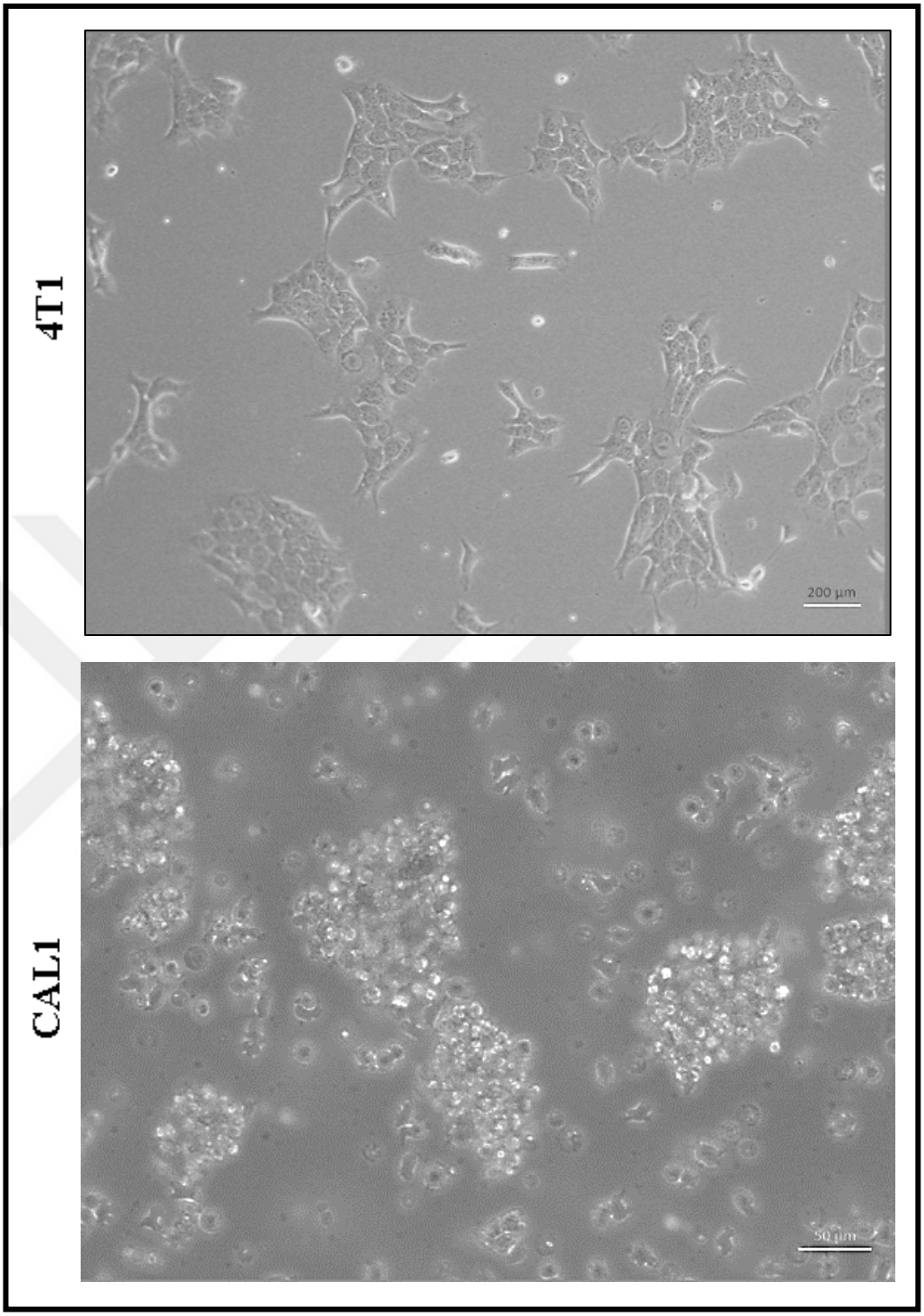

Figure 3.1 Inverted light microscope image of 4T1 and CAL1 cell lines

3.2.2 PTT and PDT protocol

Day1: The 4T1 breast cancer cells were plated onto 96-well plates ($4X10^3$ cells per well) with a volume of 100 µl.

Day2: Following overnight incubation, the wells were aspirated to remove the medium, and the cells were treated with varying doses of MXene, a photosensitive agent, in fresh media. The treated cells were then placed in an incubator set at 37°C and 5% CO_2 for 4 hours. Subsequently, the medium was aspirated, and 100 µl of fresh medium was added to each well. The 96-well plates were then subjected to light exposure for 1 hour. Refer to Figure 3.2 for an illustration of the PTT&PDT protocol.

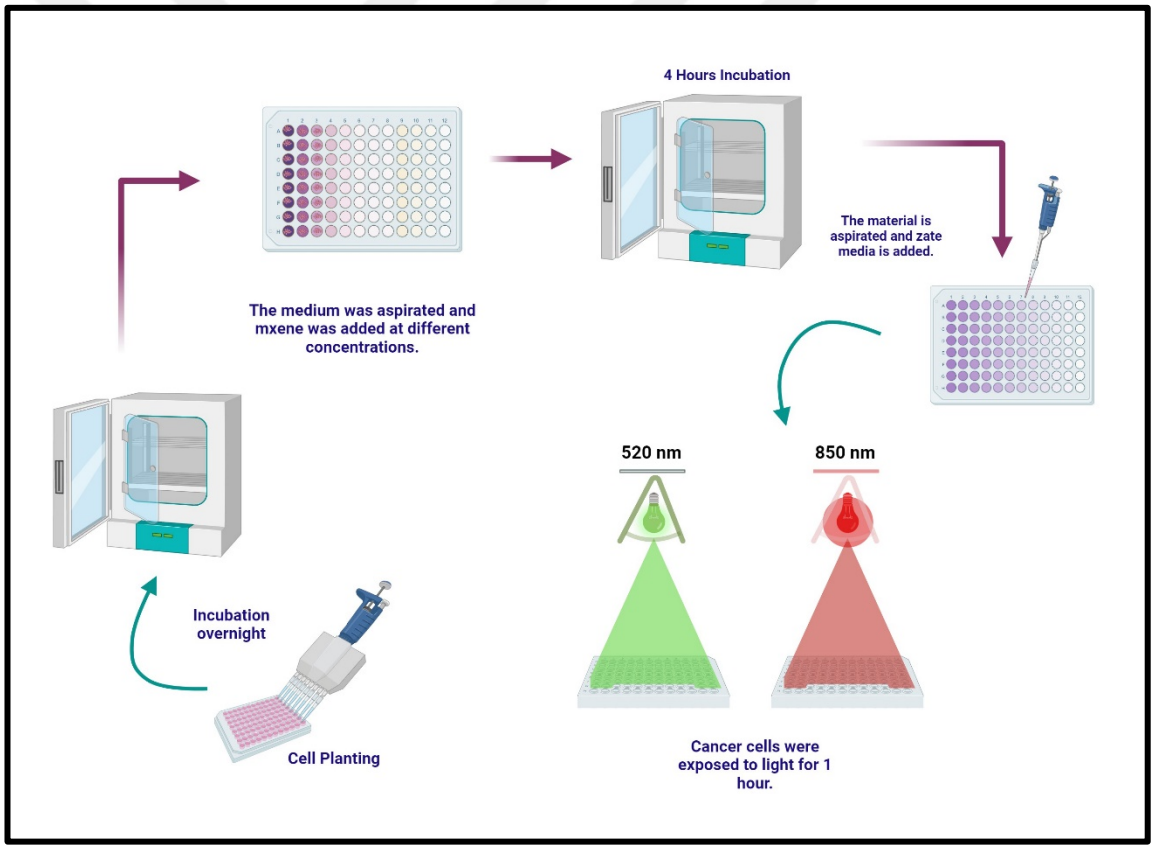

Figure 3.2. Illustration of PTT&PDT protocol

3.2.3 LDH protocol

The LDH assay is a frequently used method for evaluating cell viability or cytotoxicity (Fotakis & Timbrell, 2006). Lactate dehydrogenase (LDH) is an intracellular enzyme that is present in virtually all cells in the body. Exposure of cells to a harmful material results in the disruption of plasma membrane integrity, causing the leakage of LDH from the cells into the surrounding cell environment. LDH is a cytosolic enzyme found in many different cell types and is a well-known and reliable indicator of cellular toxicity. Damage to the plasma membrane results in the release of LDH into the cell culture medium. The liberation of this enzyme from the cell signifies cellular demise (Erkekoğlu & BAYDAR, 2021).This experiment was performed using the Thermo LDH cytotoxicity kit to evaluate the viability of cells in the presence of light and material after applying the PTT and PDT protocols and to determine the toxicity of the material.

Day 1: The 4T1 breast cancer cells were plated onto 96-well plates ($4x10^3$ cells per well) with a volume of 100 µl.

Day 2: After overnight incubation, the medium was removed from the wells, and the cells were treated with varying doses of MXene, a photosensitive agent, in fresh medium for 4 hours at 37°C and 5% CO_2 in the incubator. Following this incubation period, the medium was aspirated, and 100 µl of fresh medium was added to each well. Subsequently, the 96-well plates were exposed to light for 1 hour. Finally, the cells were further incubated for 24 hours under the same conditions.

Day 3: At the end of 24 hours, the protocol in the Thermo LDH kit started to be applied. Preparation Before LDH

- The lysis buffer, stop solution, substrate mix and assay buffer included in the kit and stored at -20 °C are brought to room temperature and allowed to melt by protecting them from light.
- To prepare the substrate stock solution, combine 11.4 ml of distilled water with the substrate mix. Then, create the reaction mix by adding 600 µl of assay buffer to the substrate stock solution.

LDH Steps

1. Add 10 µl of lysis solution per well to the incubated 96 well plates, scrape the bottom of the wells with a 1000-well pipette and pipet it, foam it and then incubate it at 37°C for 45 minutes.

2. Cells treated with lysis buffer are collected in Eppendorf according to their groups and centrifuged at 13,000 rpm for 10 minutes, and the supernatant is distributed to new wells in a volume of 50 µl per well. 50 µl reaction mix is added to the wells and the plates are incubated for 30 minutes at room temperature and in the dark.

3. At the end of the incubation, stop solution is added to the wells in a volume of 50 µl and care is taken to ensure that there are no bubbles in the wells at this stage.

4. Then, readings are taken at 490-680 nm in the microplate reader. After the reading is taken, the values read at 490 nm and 680 nm are subtracted from each other, the viability in the control group is normalized to 100% and the viability graph is drawn.

3.2.4 Optimization of proper mxene concentration and wavelength

1. 4T1 cells are seeded in a 96 well plate with 100 µl medium volume at $4x10^3$ cells per well and incubated overnight.

2. The medium of the cells kept overnight is aspirated and the cells are incubated with MXenes at the concentration specified in Table 3.3 for 4 hours. The same process is repeated for cells in the control group with fresh medium.

Tablo 3.2 Mxene types and concentrations used in the optimization phase

Mxene Types	Concentrations
$Mo_2Ti_2C_3$	50 µg/ml, 100 µg/ml, 150 µg/ml, 200 µg/ml
Nb_4C_3	50 µg/ml, 100 µg/ml, 150 µg/ml, 200 µg/ml
Ta_4C_3	50 µg/ml, 100 µg/ml, 150 µg/ml, 200 µg/ml

3. Following the 4-hour treatment of cells with various materials and concentrations of MXenes, the medium was aspirated from both the experimental and control groups.

Subsequently, 100 µl of fresh medium was added to each well of the control group, while maintaining the experimental conditions for the treated groups.

4. After adding fresh media, the 96-well plates were kept under lights at wavelengths of 520nm and 850nm for 1 hour. Cells whose PTT and PDT protocols were completed were incubated for 24 hours.

5. At the end of 24 hours, Thermo LDH cytotoxicity kit protocol was applied to the cells and cell viability graphs were drawn.

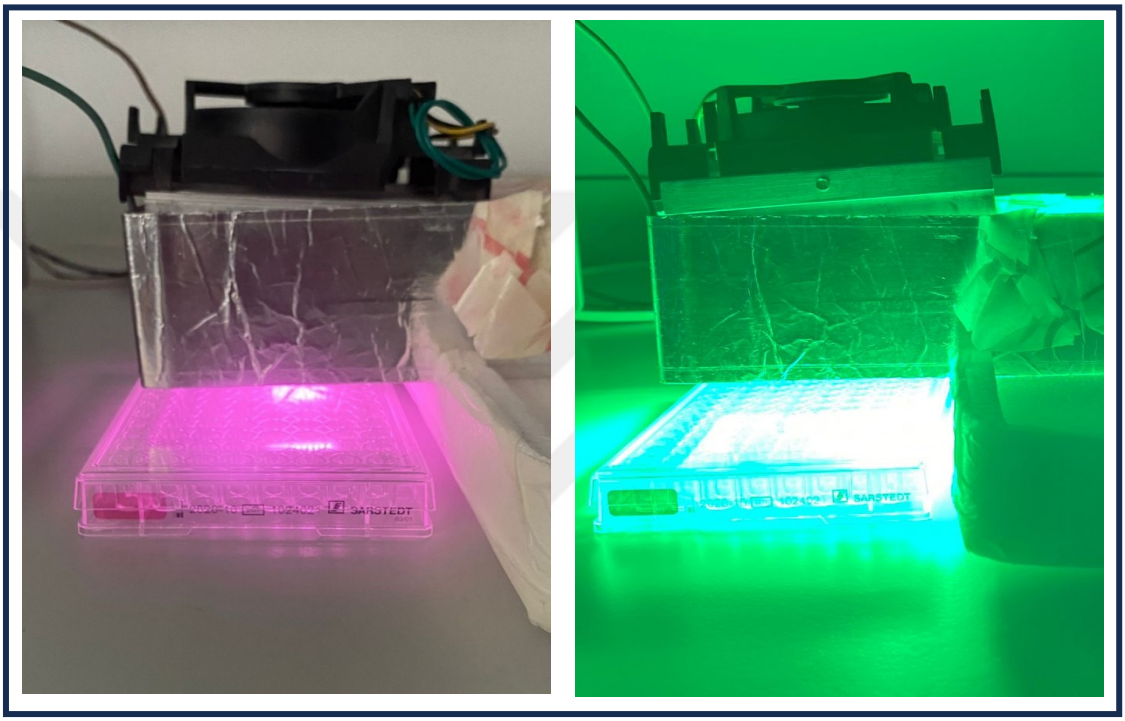

Figure 3.3 4T1 cells exposed to LED light at wavelengths of 520 nm and 850 nm

3.2.5 Optimization of light duration

The Thermo LDH cytotoxicity kit was utilized to conduct this experiment, aiming to assess the impact of varying exposure times to light on cell viability. The study examined the effects of the material in the presence and absence of PTT and PDT protocols, while also determining the material's toxicity. On the first day, 4T1 breast cancer cells were placed in 96-well plates with a volume of 100 µl per well, containing $4x10^3$ cells. On the second day, the cells were incubated overnight. The liquid in the wells was removed and the cells were then treated with a mixture containing various concentrations of MXene, a substance that aids in photosynthesis, for a duration of 4 hours. This incubation took place

in an incubator set at a temperature of 37 °C and with a CO_2 concentration of 5%. After 4 hours, the medium was removed and replaced with 100 µl of new media. The 96-well plates were then exposed to light for durations of 0.5, 1, and 2 hours. Ultimately, the cells were placed in an incubator set at a temperature of 37 °C and a CO_2 concentration of 5% for a duration of 24 hours. On the third day, when 24 hours had passed, the Thermo LDH kit routine was initiated.

3.2.6 Temperature measurement experiment

The temperature measurement experiment was carried out to determine whether there was an increase in temperature in the cells exposed to light. 4T1 Cells were treated with $Mo_2Ti_2C_3$ material at doses; 50 µg/ml, 100 µg/ml, 150 µg/ml and 200 µg/ml as described in the PTT and PDT protocol and treated under 850 nm light for 1 hour. Additionally, in addition to the 850 nm light group, a group of cells without light were treated with $Mo_2Ti_2C_3$ at doses; 50 µg/ml, 100 µg/ml, 150 µg/ml and 200 µg/ml for 4 hours in order to determine the temperature difference in the presence and absence of light. Temperature changes of the treated cells were recorded with a non-contact thermometer.

3.2.7 Examination of ROS activity

Cells continuously generate ROS through aerobic metabolism. The generation of ROS serves a crucial function in the immune system, providing protection and facilitating normal physiological processes. Cells are equipped with a robust antioxidant defense system to mitigate the excessive production of ROS. However, oxidative stress appears when ROS generation exceeds the capacity of these intrinsic antioxidant mechanisms. This oxidative stress is implicated in various human diseases like cancer, atherosclerosis, neurological disorders, and diabetes. Several techniques are available for quantifying ROS production within cells. Basic methods often utilize cell-permeable fluorescence and chemiluminescent probes. One widely used approach involves the use of DCFH-DA to directly evaluate the cellular redox status (Eruslanov & Kusmartsev, 2010). For these reasons DCFDA kit was used in this thesis to determine the levels of ROS in cancer cells. The experiments were conducted following the kit protocol.

According to protockol;

4T1 cancer cells were seeded in 24 well plates ($25x10^3$ per well) and incubated for 24 hours.At the end of 24 hours of incubation, the fresh medium was aspirated and the cells were treated with $Mo_2Ti_2C_3$ at a concentration of 200 μg/ml for 4 hours.After 4 hours, the medium containing the material was removed from the cell and the cells were washed twice with 1xBuffer diluted with distilled water at a ratio of 1:10.After washing, DCFDA solution was introduced into the cells and placed in an incubator at 37 °C for 45 minutes. In the end, the incubation, the light groups were exposed to light at a wavelength of 850 nm for 1 hour.Finally, after washing the cells twice with PBS, the cells were fixed with cold methanol for 15 minutes at -20 °C. After the fixation process, the cells to which 4',6-diamidino-2-phenylindole was dropped were examined under a fluorescent microscope for nuclear staining.

3.2.8 TEM analysis

Transmission Electron Microscopy (TEM) is a technique that employs high-energy electrons to investigate samples in thin sections for imaging purposes (C. Tang & Yang, 2017). By employing a magnification of up to one million times, the visualization of immunotherapy may be achieved by observing the phagocytosis of 4T1 cells by CAL1 cells at the nanoscale scale. This phagocytosis is a consequence of PTT, and it also involves the internalization of the $Mo_2Ti_2C_3$ material by the cell. GM-CSF is a cytokine known for its role in promoting the growth and maturation of myeloid cells, aiding in the differentiation of dendritic cells, and fostering their survival in vitro (Hamilton, 2008). The following steps were followed to perform TEM analysis.

First of all, CAL1 cells were stimulated with 10 ng/ml GM-CSF for 72 hours so that CAL1 cells could mature and phagocytose 4T1 cells. After Cal 1 cells were stimulated on the first day, 4T1 cells were planted in T25 flasks at 60% occupancy ($1x10^6$) and incubated overnight. To visualize the interaction mechanism of cancer cells with the material after incubation, 4T1 cells were treated with $Mo_2Ti_2C_3$ with a concentration of

200 μg/ml for 4 hours, and then the material was aspirated and the cells were incubated with fresh medium for 2 hours. In order to visualize that CAL1 cells phagocytosed 4T1 cells, 4T1 cells were treated with $Mo_2Ti_2C_3$ at a concentration of 200 μg/ml for 4 hours, and then the material was aspirated and the cells added to fresh media were exposed to light at a wavelength of 850 nm for 1 hour. Then, 4T1 cells were cocultured with CAL1 cells stimulated with GM-CSF for 72 hours at a ratio of 1:5 (1: 4T1, 5: CAL1) and incubated for 2 hours. After 2 hours, the cells were collected by scraping with a cell scraper without aspirating the medium and transferred to the falcon. Glutaraldehyde was added to the cell suspension at a ratio of 1:1 (Glutaraldehyde must be at the same temperature as the cell, 37 °C). It was kept at room temperature for 10-15 minutes. Then, the falcones were centrifuged at 1000 rpm for 5 minutes. After centrifugation, the supernatant was withdrawn and fresh glutaraldehyde was added to the pellet. The centrifugation process was repeated and the supernatant was aspirated and fresh glutaraldehyde was added again and stored at +4 °C. The stored pellets were later delivered to Ankara University Faculty of Medicine to be examined by TEM.

3.2.9 Statistical analysis

Data analysis was conducted utilizing GraphPad Prism software (version 10). Analyses of variance (ANOVA) were conducted, followed by Tukey's multiple comparison test or Student's t-test as appropriate. Results are presented as mean ± standard deviation both numerically and graphically. Statistical significance was considered at $p < 0.05$. The sample size (n) for each experiment is specified in the respective figure legends.

4. RESULTS

4.1 Determination of Appropriate Material Concentration and Wavelength

This experiment was carried out using LDH assay to measure and compare the viability of 4T1 breast cancer cells after PTT&PDT protocol with different materials and concentrations of materials, 520 nm and 850 nm wavelength lights. During the study, all groups were evaluated numerically in terms of cell viability and the material that reduced the viability of cancer cells the most, the concentration of the material and the light at the most appropriate wavelength for the PTT&PDT protocol were determined.

4T1 cancer cells were seeded in 96 well plates ($4x10^3$ per well) and incubated overnight in an incubator at 37 °C and 5% CO_2 concentration. At the end of incubation, cancer cells were treated with different concentrations of $Mo_2Ti_2C_3$, Nb_4C_3 and Ta_4C_3 materials (50 µg/ml, 100 µg/ml, 150 µg/ml and 200 µg/ml) for 4 hours. Then, the media were aspirated and fresh media were added to the wells and exposed to light groups 520 nm and 850 nm wavelengths for 1 hour. After 24 hours, Thermo LDH kit protocols were applied and cell viabilities were compared. The optical density was assessed at wavelengths of 490 nm and 680 nm.

The viability of 4T1 cells between the $Mo_2Ti_2C_3$-treated groups compared to the no light group was compared in Figure 4.1. According to the results of the analysis, cell viability was significantly decreased in the group treated with molybdenum at a concentration of 200 µg/ml and illuminated at 850 nm wavelength compared to the no light group. According to statistical analyses, cell viability was significantly decreased in all groups treated with molybdenum.

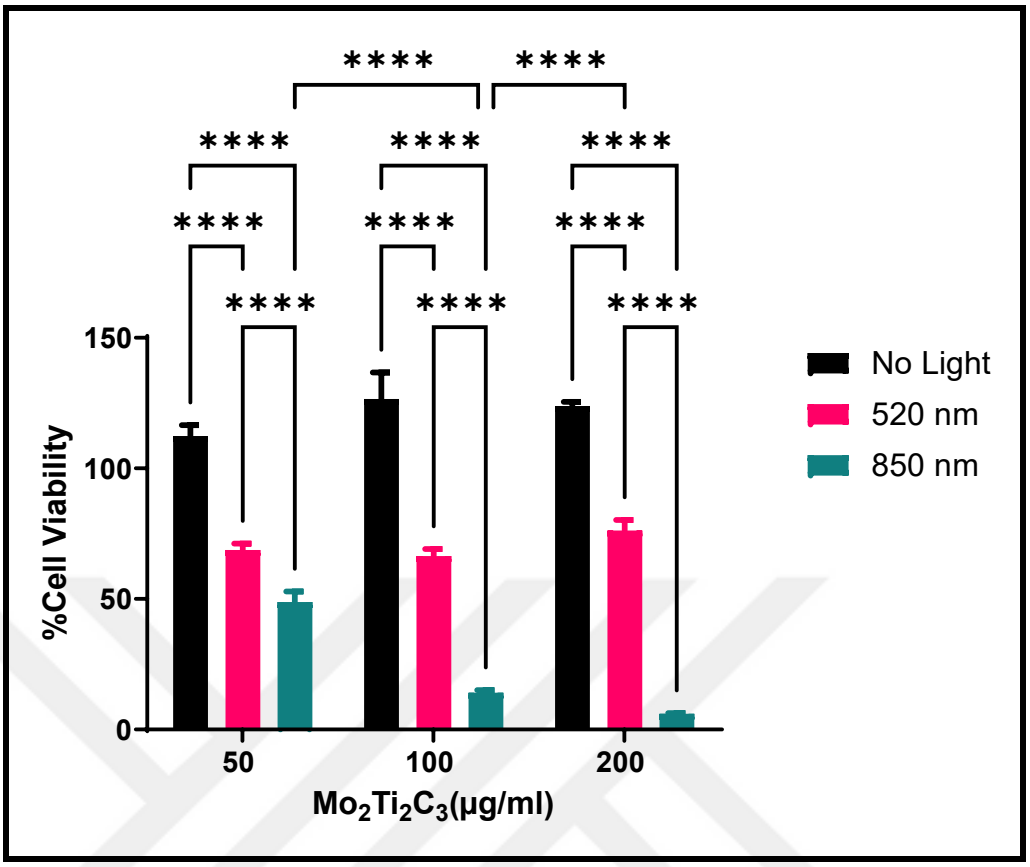

Figure 4.1 Cell viability of 4T1 cells. Viability of cells treated with $Mo_2Ti_2C_3$ after PTT & PDT protocol (n=5, ****P value <0,0001)

The cell viability between the groups treated with Nb_4C_3 and Ta_4C_3 materials was analysed in Figure 4.2 and Figure 4.3. When the cell viability of the Nb_4C_3-treated group was compared, significant decrease in cell viability was observed in the group with 100 µg/ml concentration and 850 nm light, but this decrease was not sufficient compared to the $Mo_2Ti_2C_3$ group. When cell viability was evaluated in the tantalum-treated group, no significant decrease was observed between the no-light and 850 nm light groups in the group treated with 100 µg/ml concentration.

In a study conducted by Liu et al., a composite MXene known as Ta_4C_3-IONP-SPs was developed for the treatment of breast cancer. This composite MXene integrates tantalum (Ta_4C_3) MXene with a surface superparamagnetic iron oxide functionalization for enhanced efficacy.In the PTT study with Ta_4C_3-IONP-SPs composite MXene, in vitro cell viability was evaluated in the 4T1 cell line and tumour size was found to be reduced

in the in vivo study (Z. Liu, Lin, et al., 2018). However, in the Ta_4C_3-treated group, contrary to expectations, it was observed that cancer cell viability increased in the group treated with light at a concentration of 100 µg / ml and 520 nm wavelength.

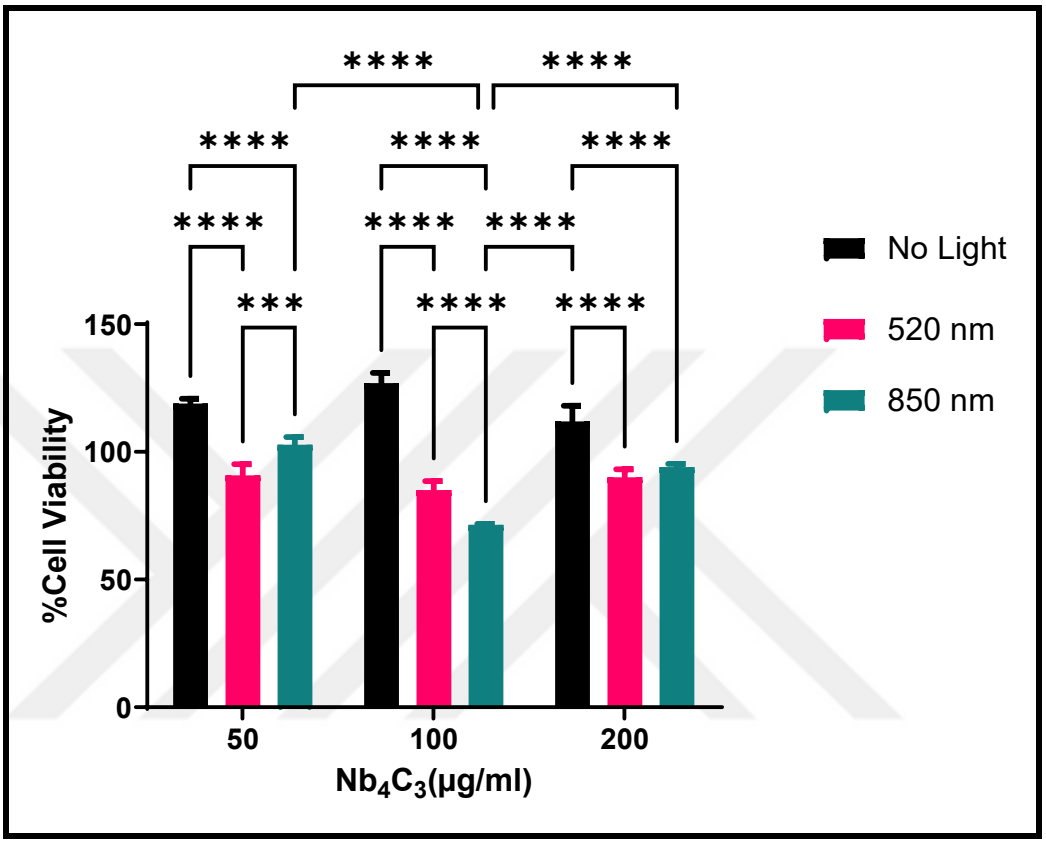

Figure 4.2 Cell viability of 4T1 cells. Viability of cells treated with Nb_4C_3after PTT & PDT protocol (n=5, ***P value=0,0001, ****P value <0,0001,)

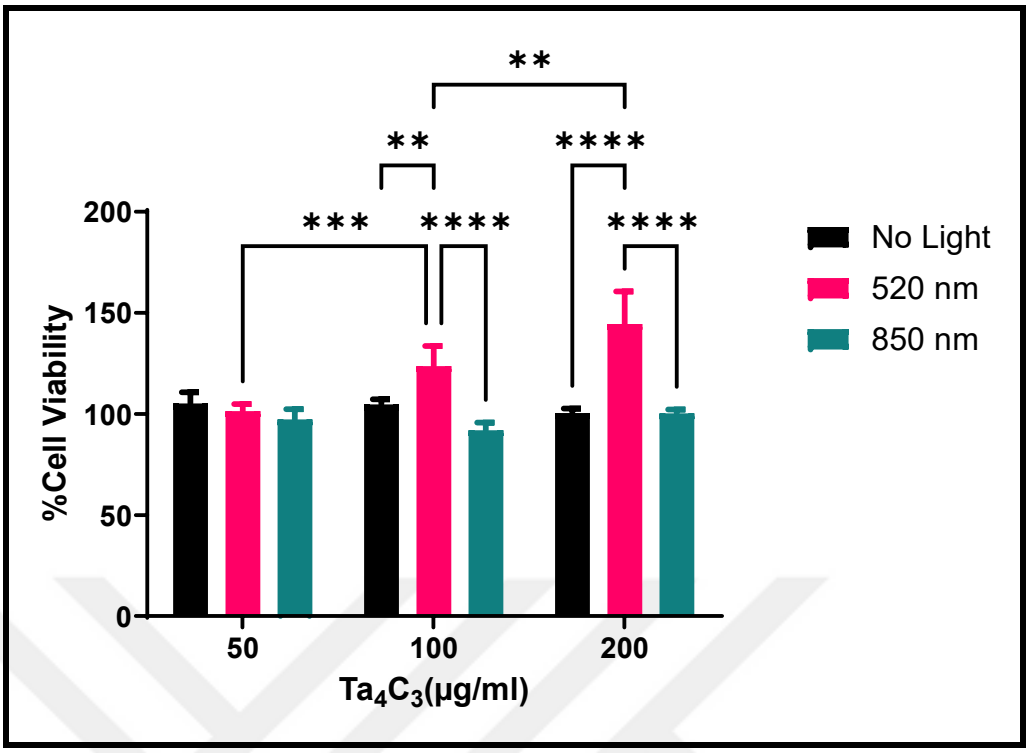

Figure 4.3 Cell viability of 4T1 cells. Viability of cells treated with Ta_4C_3 after PTT & PDT protocol (n=5, **p value=0,0044, ***=0,005, P value ****P value <0,0001)

As a result, at this stage of the thesis, it was determined that $Mo_2Ti_2C_3$ decreased cell viability at a very high rate compared to other materials. In addition, when the previous PTT and PDT studies (Table 2.2) were examined, it was decided to use $Mo_2Ti_2C_3$, which had not been used for PTT & PDT protocols before, as a photosensitiser at a concentration of 200 µg/ml (Figure 4.1).

4.2 Determination of Light Exposure Time

During this phase of the thesis, 4T1 cells treated with $Mo_2Ti_2C_3$ were subjected to varying durations of light exposure to determine the optimal exposure time using the Thermo LDH cytotoxicity kit. Initially, 4T1 cells were seeded into 96-well plates at a density of $4x10^3$ cells per well and allowed to incubate overnight at 37 °C and 5% CO_2. Following the overnight incubation, the cells were exposed to media containing $Mo_2Ti_2C_3$ at a concentration of 200 µg/ml for a duration of 4 hours. Subsequently, the media containing the material was removed, and fresh media was added to the wells. The cells were then

subjected to LED light with a wavelength of 850 nm for durations of 0.5, 1, and 2 hours to determine the optimal exposure time yielding the highest mortality rate. After 24 hours following this procedure, cell viability in the presence of material and light was assessed using the LDH assay.

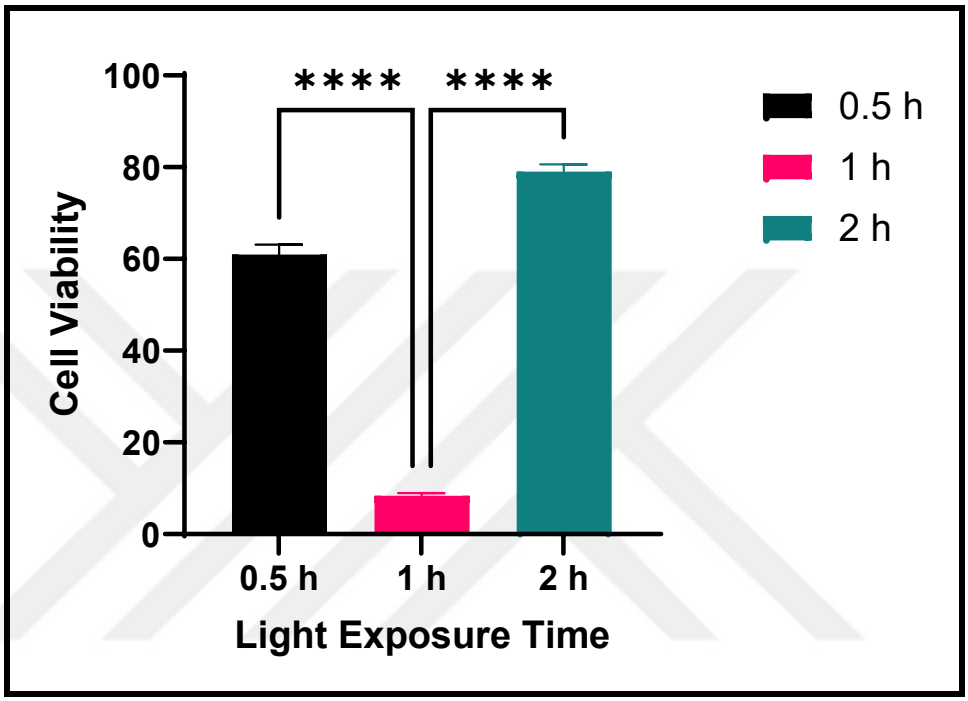

Figure 4.4 4T1 cells were treated with $Mo_2Ti_2C_3$ at a concentration of 200 µg/ml for 4 hours followed by evaluation of cell viability in the presence of 850 nm led light for 0.5, 1 and 2 hours (n=5, ****P value <0,0001)

Cell viability of cells treated with $Mo_2Ti_2C_3$ at a concentration of 200 µg/ml in the presence of 850 nm led light for 0.5, 1 and 2 hours is shown in Figure 4.4. During the experiment, the viability of the control groups was also analysed for each light duration group (0.5, 1 and 2 hours). However, since the LDH kit was used to analyse the cell viability in this experiment, the control group of each group was normalised to 100% and the control group was not shown in the graph. When the light exposure times were examined, it was found that the decrease in cell viability was noticeably in the group exposed to light for 1 hour and there was a significant difference between the groups when the groups were evaluated in terms of cell viability.

4.3 Temperature Measurement Experiment

Phototherapy, often known as PTT, is an advanced technology used in the treatment of cancer. PTT, or photothermal therapy, is a minimally invasive and potentially beneficial approach for the treatment of cancer. PTT is a procedure that involves employing laser light in the near-infrared (NIR) range to activate photosensitizing chemicals. This activation generates heat, which is then used to selectively destroy cancerous tumors while minimizing damage to the surrounding healthy tissues (Bhole, Bonde, Kadam, & Wavwale, 2021).

The temperature measurement experiment performed at this stage of the thesis was carried out to determine the increase in cell temperature following the PTT&PDT protocol. It is also to prove that the treatment method is PTT. For the temperature measurement experiment, 4T1 cells were seeded in 96 well plates ($4x10^3$ per well). As in the PTT&PDT protocol, the cells were incubated overnight in an incubator at 37 °C and 5% CO_2 concentration. At the end of incubation, the medium was aspirated and the cells were incubated with medium containing $Mo_2Ti_2C_3$at concentrations of 50 µg/ml, 100 µg/ml and 200 µg/ml for 4 hours at 37 °C. At the end of 4 hours, the well temperatures in the no light group were measured and recorded with a non-contact thermometer from the well where the material concentration was high to the well where it was low. In the light groups, after 4 hours of incubation, the medium with material was aspirated, fresh medium was added to the wells and the plate was exposed to led light at 850 nm wavelength for 1 hour. Cell temperatures in the wells exposed to light were measured and recorded as in the no light group without allowing the plate to cool down at the end of 1 hour.

The graph drawn with the recorded temperatures is shown in figure 4.5. While the recorded temperatures were shown in the graph, a control group was added separately for each concentration group in order to see the difference better. While analysing the recorded temperatures, the mean value of the temperatures in each group was calculated. Then the difference between the average value of each group and the control groups was taken and the graph was drawn. For this reason, since the temperature change in the

control groups would be 0, the control group was not shown in the graph.As a result of the experiment, an increase in temperature between no light and light group was determined. At the same time, it was determined that the temperature increase in the light group increased depending on the material concentration. Thus, it was proved that $Mo_2Ti_2C_3$ showed photothermal effect under 850 nm led light.

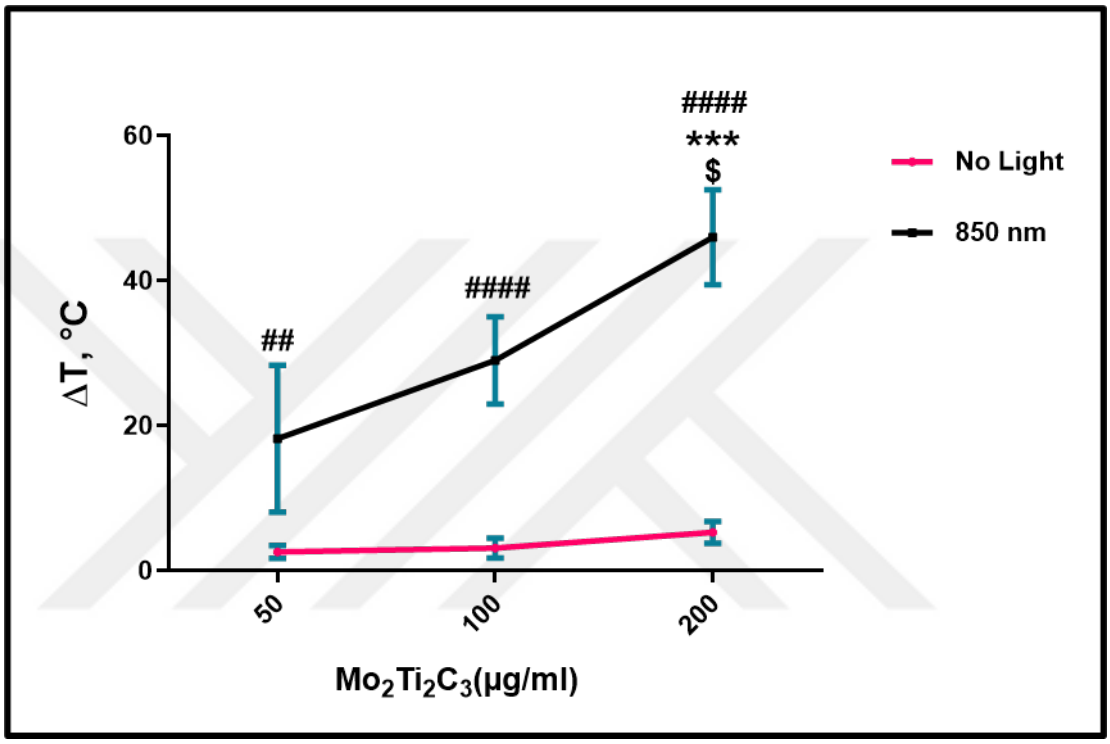

Figure 4.5 The temperature rise following treatment of 4T1 cells with $Mo_2Ti_2C_3$ at a concentration of 200 µg/ml for 4 hours was recorded using a non-contact temperature meter (n=5, $ P value <0,0001 versus 850 nm 50 µg/ml, ***P value=0,0009 versus 850 nm 100 µg/ml, #####P valuve <0,0001 versus no light)

4.4 Examination of ROS Activity

PDT stands as a highly promising approach in cancer therapy, offering significant efficacy. The method involves administering a tumor-targeted photosensitizer into the patient's system, followed by direct tissue irradiation using a laser, resulting in notable tumor ablation effects(J. Chen et al., 2020). PDT induces the production of ROS through photochemical processes. PDT might potentially enhance the generation of ROS via

modifying metabolism, inducing endoplasmic reticulum stress, or affecting the mitochondrial membrane potential (Z.-J. Zhang, Wang, Mo, Xiong, & Wen, 2020).

This experiment utilized DCFDA, fluorogenic dye, to assess hydroxyl, peroxyl, also ROS activity in the cell. Upon penetration into the cell, DCFDA undergoes oxidation by reactive oxygen species to form DCF. The DCFDA kit was employed to quantify ROS levels in the cells. 4T1 cells were seeded in 24-well plates 25,000 cells per well and incubated overnight in a CO_2 incubator at 37°C. Subsequently, the media were aspirated, and the cells were incubated with media containing DCFDA at a concentration of 200 µg/ml for 4 hours. Following incubation, ROS activity in the treated cells was examined using a fluorescence microscope according to the DCFDA kit protocol, with the light-exposed groups subjected to 850 nm light for 1 hour. By applying this method, cell nuclei appear blue and oxidative stress cells appear green in fluorescence microscope. Fluorescence microscope images are shown in figure 4.6.

In the naive group, only 4T1 cells have DAPI images. In other words, there are nucleus images without any treatment after the cells are seeded. In the $Mo_2Ti_2C_3$ group, after the cells were treated with the material, both DAPI for nuclei staining and FITC images for ROS detection were taken. In the $Mo_2Ti_2C_3$+Light group, after the cells were treated with the material, both DAPI and FITC channel images were taken by exposing the cells to light at 850 nm wavelength for 1 hour. As seen in Table 2.2, we did not expect ROS release in 4T1 cells exposed to light at 850 nm wavelength since MXenes showed PTT therapy effect at 808 nm wavelength. As seen in Figure 4.6, ROS emission was not detected in the FITC channel.

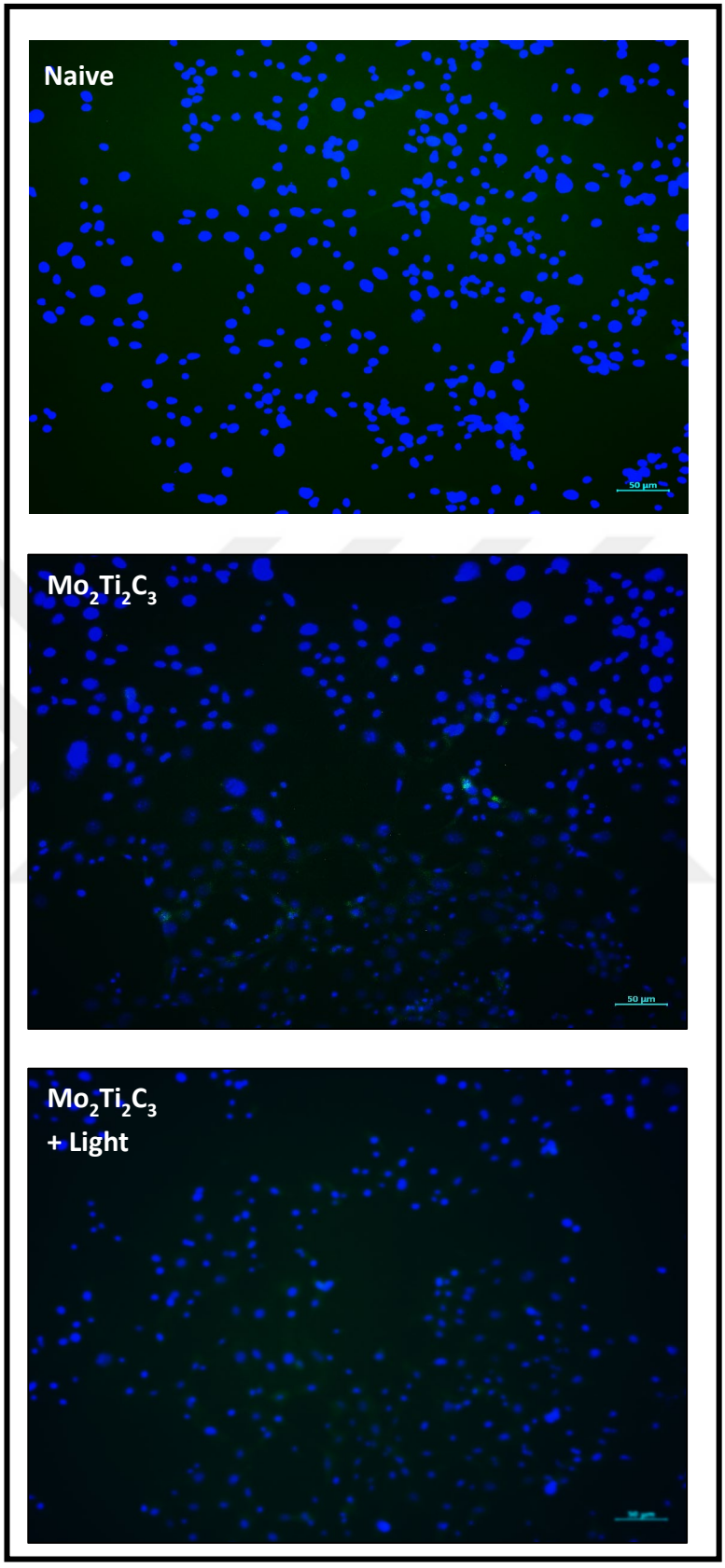

Figure 4.6 Fluorescence microscope images of ROS activity after PTT&PDT protocol applied to 4T1 cells

4.5 TEM Analysis

Immunotherapy utilizes the body's immune system to identify and combat cancer cells. Shows remarkable potential in treating various cancers, especially aggressive and metastatic forms (Z. Xu et al., 2013). Cancer immunotherapy depends on the effective display of tumor antigens to T-cells in order to provoke a strong anti-tumor immune response and establish durable immunological memory. This process leads to the destruction of cancer cells and the prevention of cancer recurrence (Paulis et al., 2013).

The combined use of immunotherapy and PTT for cancer treatment has many advantages. For example, nanomaterial-driven photothermal therapy (PTT) not only eradicates the primary tumor but also stimulates immune responses by promoting immunogenic cell death (ICD) through hyperthermia induced by PTT (refer to Figure 4.7). Moreover, these engineered nanoplatforms can be readily internalized by dendritic cells (DCs) through endocytosis. Beyond addressing primary tumors, they have the potential to establish durable immune memory, mitigating the risk of cancer metastasis and recurrence (Huang, Lu, Guo, Du, & Han, 2021).

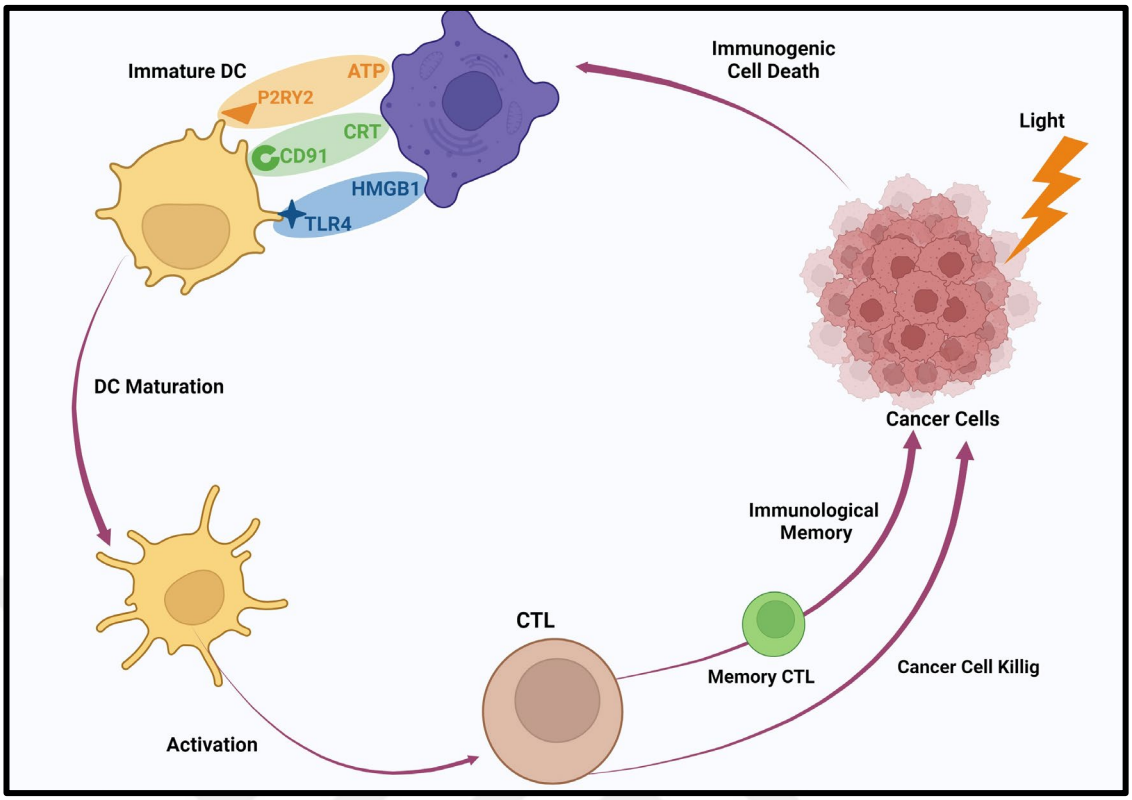

Figure 4.7 Schematic representation of PTT triggering ICD

TEM analysis was performed to show the passage of the nanomaterial through the plasma membrane, as well as to show that PTT induces ICD induction and immunotherapy. This experiment can be performed by flow analysis if the material has fluorescent properties, but since $Mo_2Ti_2C_3$ does not have fluorescent properties, TEM analysis method was used.

To see the differences between the groups, only the group containing CAL1 cells was examined under TEM microscope. TEM images of CAL1 cells are shown in Figure 4.8.

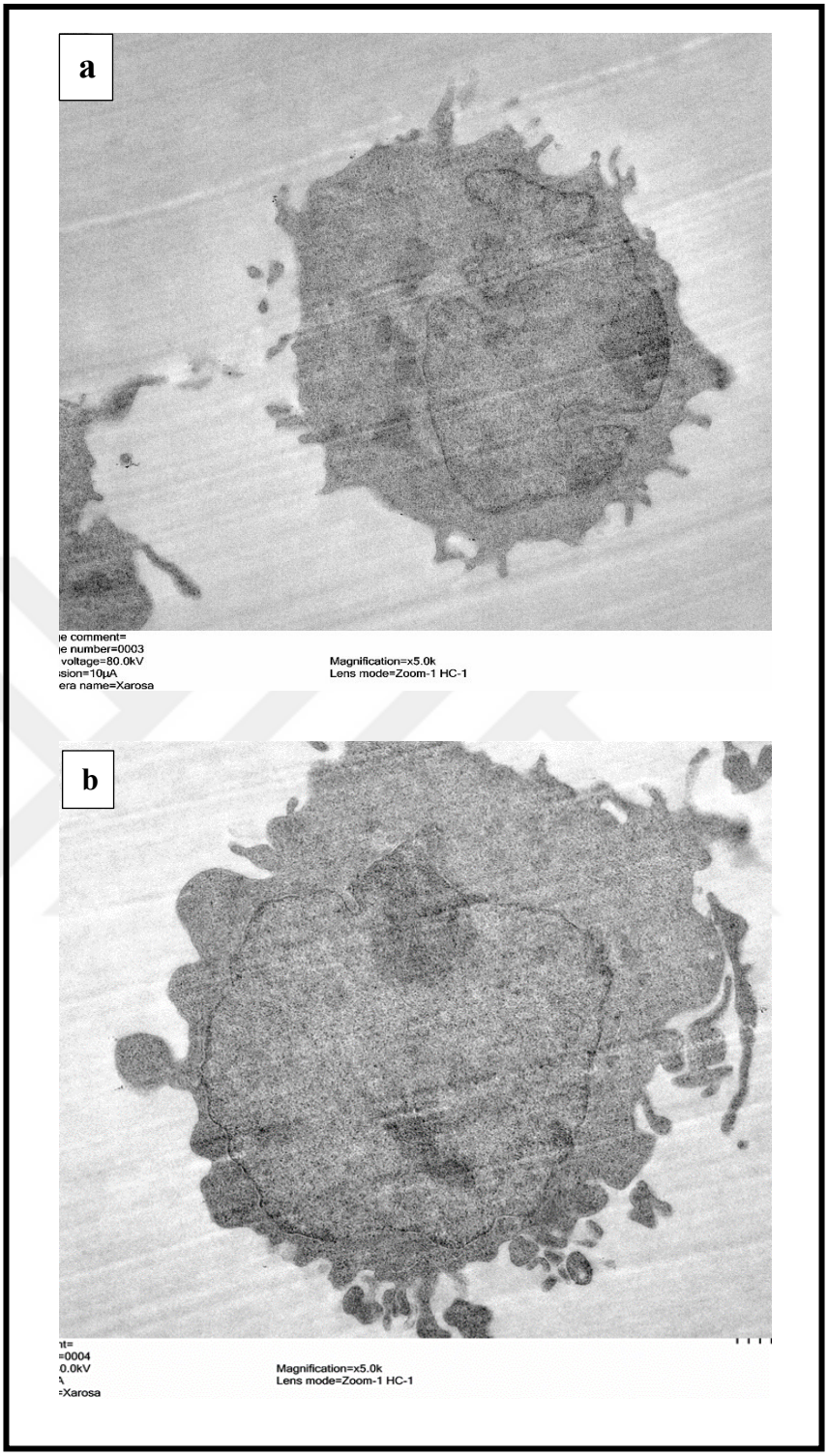

Figure 4.8 TEM imaging of CAL1 cells
(Magnifications: a=2.0 µm, b=2.0 µm)

In order to demonstrate that CAL1 cells take up the material into the cell by endocytosis, cells stimulated with GM-CSF for 72 hours were treated with media containing $Mo_2Ti_2C_3$ at a concentration of 200 µg/ml for 2 hours. They were then prepared for TEM imaging. The endocytosis of the material by CAL1 is shown in Figure 4.9.

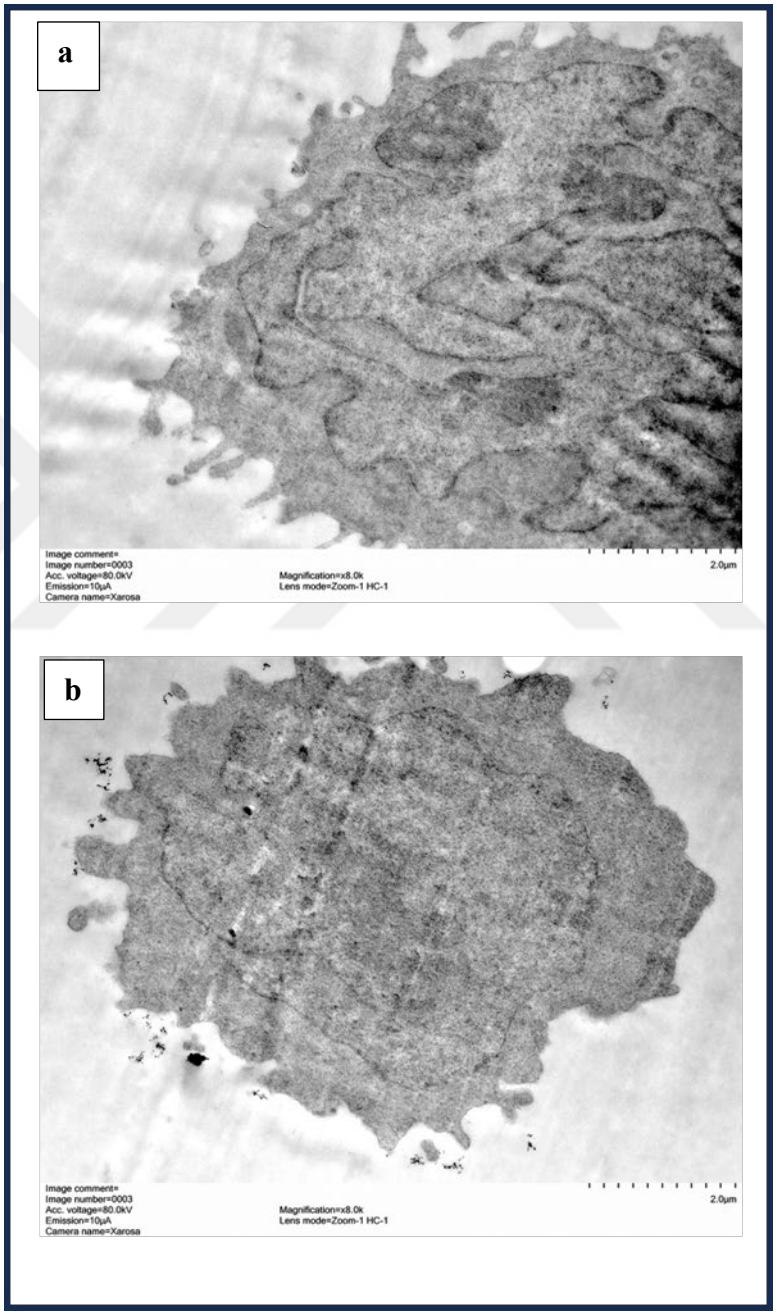

Figure 4.9 TEM imaging of endocytosis of material by CAL1
(Magnifications: a=2.0 µm, b=2.0 µm)

To demonstrate the intracellular passage of 4T1 cells through the endocytic pathway, 4T1 cells were seeded in T25 flasks at 60% occupancy. After overnight incubation at 37°C in a 5% CO_2 atmosphere, the seeded cells were subjected to treatment with $Mo_2Ti_2C_3$ at a concentration of 200 µg/ml for 4 hours the following day. Subsequently, they were prepared for TEM imaging. The migration of the material through 4T1 cells is illustrated in Figure 4.10, Figure 4.11, and Figure 4.12.

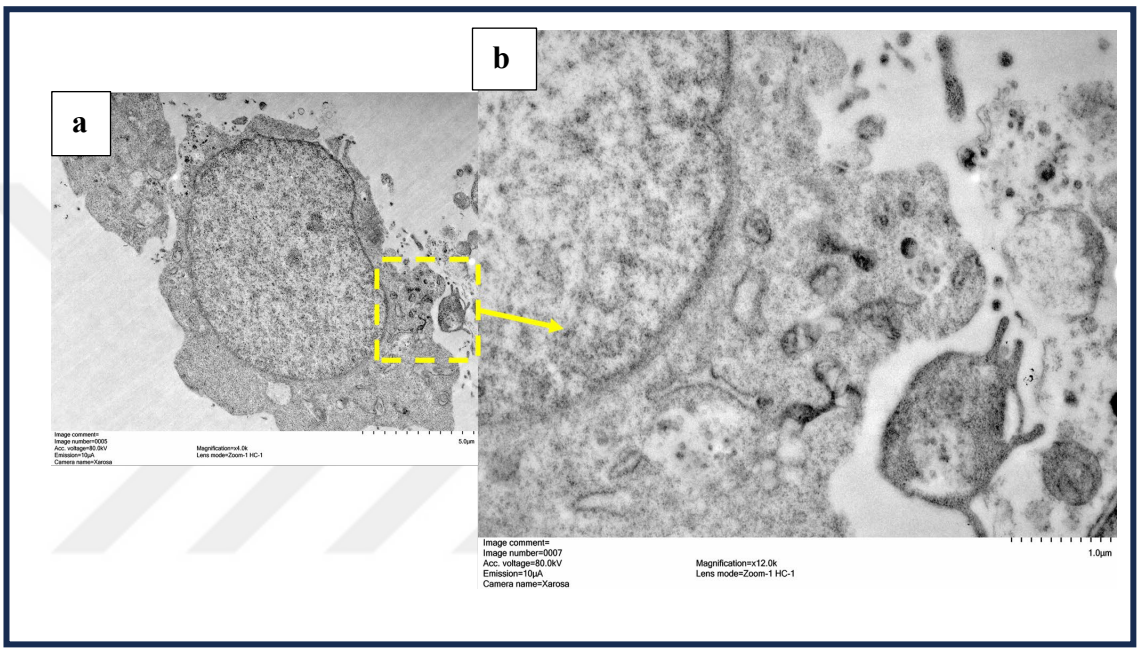

Figure 4.10 TEM imaging of $Mo_2Ti_2C_3$ treated 4T1 cells show the material uptake via endocytic pathway (Magnifications: a=2.0 µm, b=2.0 µm)

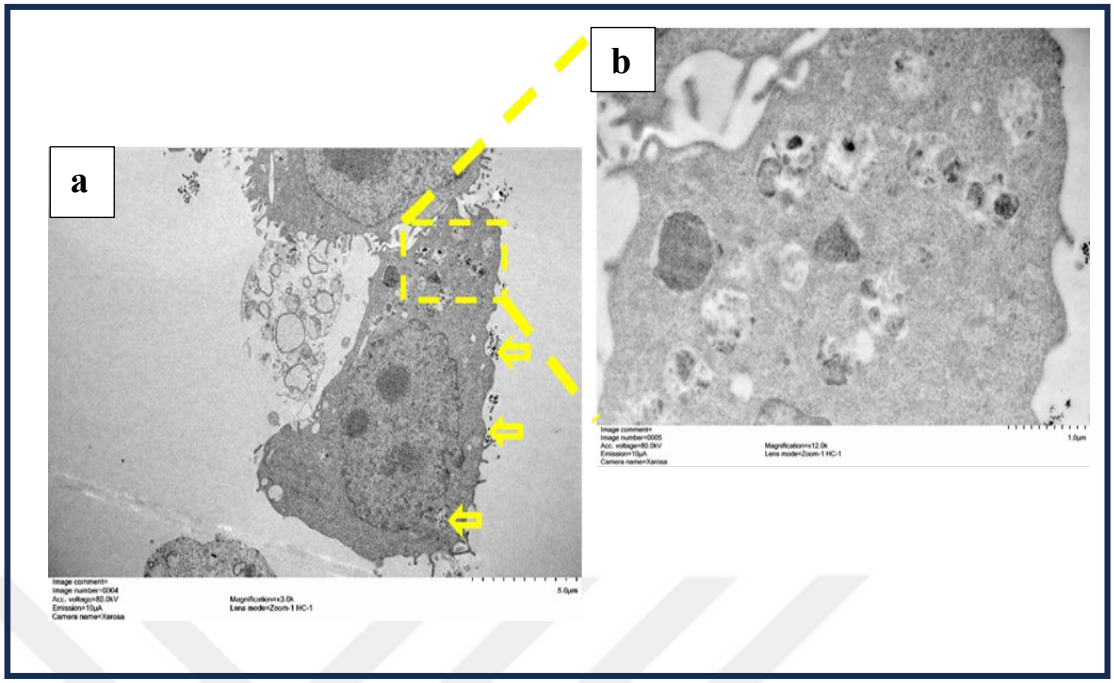

Figure 4.11 TEM imaging of $Mo_2Ti_2C_3$ treated 4T1 cells show the material uptake via endocytic pathway. (Magnifications: a=5.0 µm, b=1.0 µm)

In order to see the immuno-therapeutic effect of PTT, CAL1 cells were stimulated with GM-CSF for 72 hours and their maturation was supported. 4T1 cells were seeded into T25 flasks at 60% confluence in the same way and incubated in the incubator for 1 night. At the same time, after incubation, they were treated with media containing $Mo_2Ti_2C_3$ at a concentration of 200 µg/ml for 4 hours. Afterwards, the media was removed from the flasks and fresh media was put then the cancer cells were exposed to 850 nm wavelength light for 1 hour. After 4T1 cells were cocultured with GM-CSF-stimulated CAL1 cells at a ratio of 1:5 (1:4T1, 5:CAL1) and incubated for 2 hours, the cells were prepared for TEM analysis. It is shown in Figure 4.12 and Figure 4.13 that CAL1 cells phagocytose materials after PTT treatment.

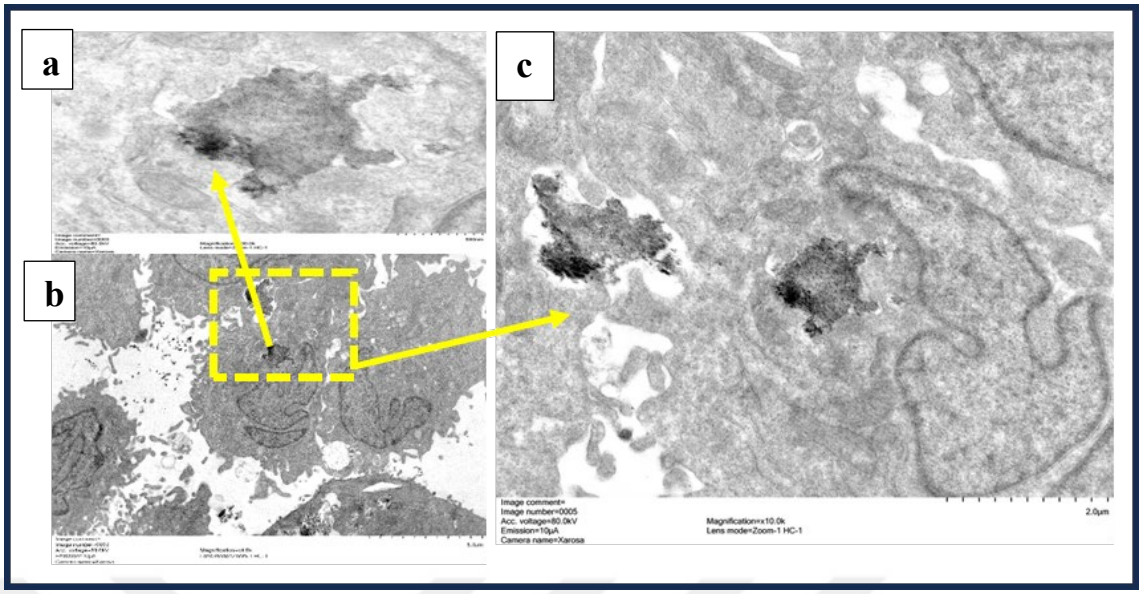

Figure 4.12 TEM imaging of phagocytosis of materials by CAL1 cells after PTT triggered immunotherapy (Magnifications: a=500nm, b=5.0µm, c=2.0 µm)

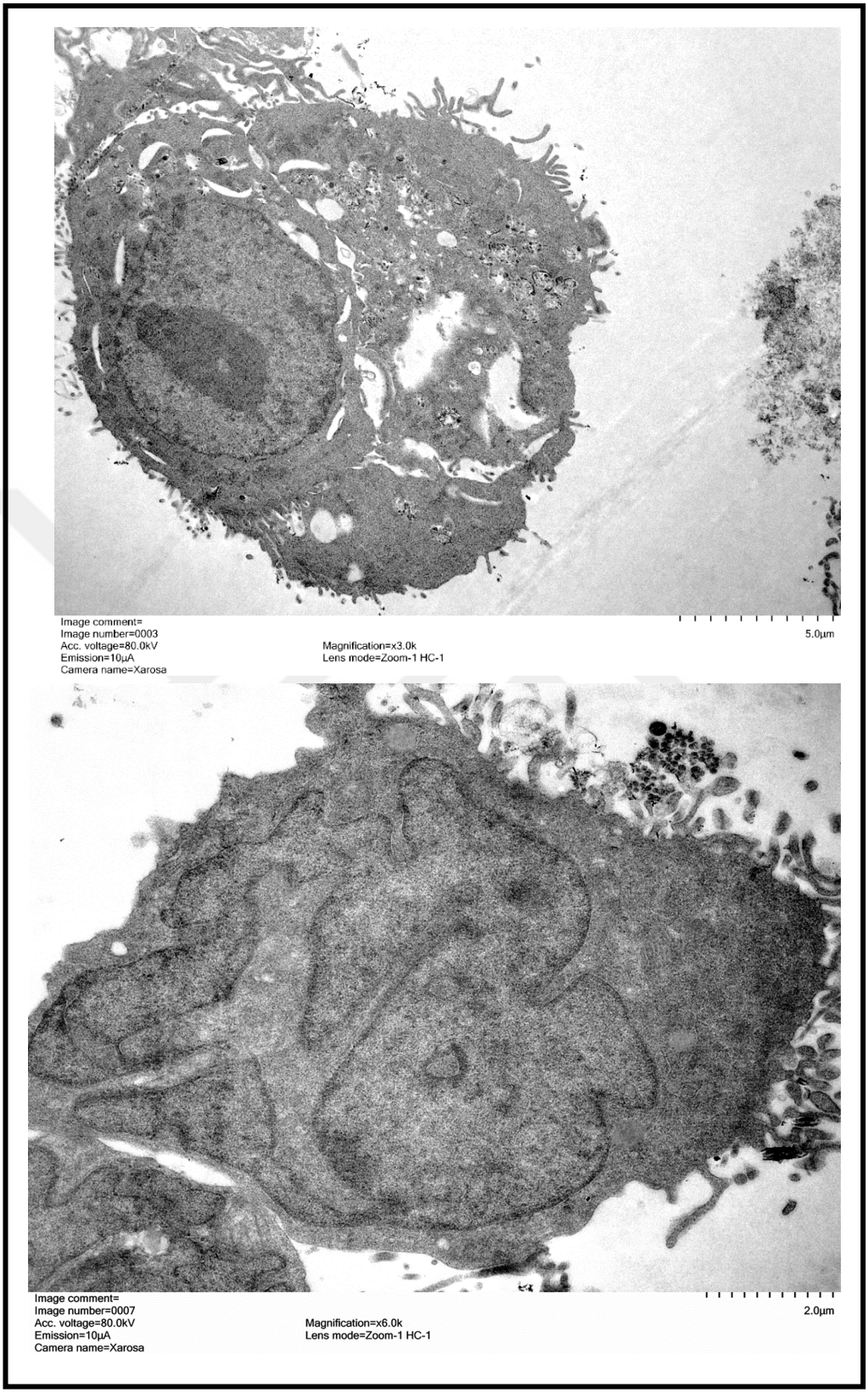

Figure 4.13 Material uptake of CAL1 cells after the PTT protocol

When Figure 4.11 and Figure 4.12 are compared, it is seen that the structures enclosed in the cell are different. It is not possible to clearly identify these structures by TEM analysis alone. However, it can be considered that the structure enclosed in the cell in Figure 4.12 is a more complex structure consisting of cellular debris and material. TEM analysis has shown that PTT using $Mo_2Ti_2C_3$ induces immunotherapeutic effect by triggering ICD.

5. DISCUSSION

Since their introduction in 2011, MXenes have emerged as a distinct class of two-dimensional (2D) materials characterized by stratified configurations of early transition metal atoms linked by a layer of carbon or nitrogen atoms. These materials fall into categories such as transition metal carbides, nitrides, or carbonitrides(Naguib et al., 2011). Molybdenum (Mo) is an essential trace element in the human diet, vital for various metabolic processes crucial to human health. Enzymes containing molybdenum are integral to key metabolic pathways within the body. In biomedical research, molybdenum-based nanomaterials (Mo-NMs), including nanocomposites, polyoxometalates, molybdenum dichalcogenides, and molybdenum oxides, have garnered significant attention for their exclusive chemical and physical properties. Their remarkable biocompatibility and degradability make them promising candidates for applications such as PTT(Z. Zhou et al., 2022). In this thesis study, the effects of PTT and immunotherapy made with $Mo_2Ti_2C_3$ nanomaterial containing Molybdenum, which is one of the derivatives of MXene, on breast cancer were investigated by using it in combination.

Firstly, 4T1 breast cancer cells were treated with different concentrations of MXene and PTT & PDT protocols were applied by exposing the cells to different wavelengths of light for 1 hour and cell viability was measured. According to cell viability assays, the best cell death was found in the groups treated with $Mo_2Ti_2C_3$ at a concentration of 200 μg/ml and exposed to led light at 850 nm wavelength.The viability of 4T1 breast cancer cells among the $Mo_2Ti_2C_3$-treated groups compared to the non-illuminated group is compared in Figure 4.1. Then, in order to determine the light exposure time at which the best cell death occurs, the groups were treated with 200 ug/ml $Mo_2Ti_2C_3$, under the control of each group, and one group was exposed to LED light for 30 min, one group for 1 hour and the other group for 2 hours. After 24 hours, LDH analysis was performed to determine cell viability. As shown in Figure 4.4, the best mortality rate was in the group exposed to 1 hour of light. However, it was observed that the viability of the cells exposed to 2 hours of light increased significantly. This may suggest that the 2-hour period may have allowed the cells to proliferate.

Temperature measurement and ROS analyses experiments were performed to determine whether the protocol applied was PTT or PDT protocol. As shown in Figure 4.5, it was determined that there was a concentration-dependent temperature increase in the groups treated with different concentrations of $Mo_2Ti_2C_3$ and exposed to light at 850 nm wavelength. In the ROS examination experiments, no ROS increase was detected and it was supported that the applied protocol was PTT like in literature. For example, Li et al. developed a new composite material combining MnO_2 with two-dimensional material Ti_3C_2 for the first time and aimed to treat cancer by using the composites, PTT and CDT together. In their study results, they suggested that the photothermal properties of the materials under 808 nm laser irradiation not only destroy tumour cells using local high temperature, but also enhance CDT effects. In the temperature measurement experiments, they determined that the cell temperature of PTT application with this new structure increased up to 60.8 °C (J. Li et al., 2022).For example, in one of the PTT applications of Ti_3C_2, the photothermal effect of MXene due to laser irradiation was monitored with an infrared camera and the photothermal effect of the material was demonstrated, but ROS analysis was not performed since ROS release was not expected at this wavelength (Kyrylenko et al., 2022). In a separate study conducted by Zhang et al., Mo_2C was employed as a theranostic agent and imaging contrast agent for tumor phototherapy. The experiments demonstrated that Mo_2C had a broad and intense absorption in both the visible and near-infrared (NIR) regions as a result of its metalloid characteristic when exposed to a 1064 nm laser. Furthermore, it was shown that the material induced hyperthermia and ROS formation (Q. Zhang et al., 2019).

TEM analysis was performed to demonstrate the transition of the nanomaterial through the plasma membrane, as well as that PTT induces ICD induction and immunotherapy. After PTT, the CAL1 cell line was used as a dendritic cell to show that immunotherapy was triggered and cancer cells were phagocytosed by dendritic cells as in immunotherapy. For TEM analyses, only CAL1 cells, CAL1-cells treated with material, PTT-protocol-treated 4T1 breast cancer cells and 4T1-Cells made from PTT co-cultivated with CAL-1 cells were examined under TEM in order to determine whether post-PTT ICD was triggered. Comparing Figure 4.11 with Figure 4.12 reveals differences in the structures

included inside the cell. TEM investigation alone does not allow for accurate identification of these structures. The structure inside the cell in Figure 4.9 may be seen as a complicated formation of cellular detritus and substances. According to these results, it can be suggested that $Mo_2Ti_2C_3$ nanomaterial triggers ICD in the presence of PTT.

The study conducted by Sweeny et al. focused on the utilization of Prussian blue nanoparticles (PBNPs), which are organic photothermal agents, for the purpose of achieving a combination approach of photothermal-immunotherapy against neuroblastoma. Experimental findings conducted in living organisms indicated that intratumoral injection of PBNPs effectively facilitated photothermal therapy (PTT), resulting in the complete eradication of the original tumor in mice with neuroblastoma. Furthermore, they provided evidence that PTT can activate ICD, characterized by elevated CRT expression and the release of ATP and HMGB1. The findings demonstrated that PTT has the ability to not only eliminate primary tumors by inducing hyperthermia, but also stimulate the host immune system to prevent the formation of new cancers (Sweeney, Cano-Mejia, & Fernandes, 2018).

Xu et al. conducted a study utilizing Mxenes to investigate the impact of combining anti-PD-L1 antibody with UCNPs@$Ti_3C_2T_x$ on tumor inhibition. Their findings demonstrated that this combination resulted in a prolonged and enhanced tumor inhibition effect. This highlights the significance of immunotherapy in cancer treatment, as observed in their PDT study with UCNPs@Ti_3C_2Tx, a composite material created by merging upconversion nanoparticles (UCNPs) with $Ti_3C_2T_x$ (D. Xu et al., 2020).

Liu et al. pioneered the development of an innovative theranostic nanoplatform for breast cancer, utilizing tantalum carbide (Ta_4C_3) MXene and its surface-superparamagnetic iron-oxide functionalization (Ta_4C_3-IONP-SPs composite MXenes). They comprehensively assessed its efficacy in photothermal therapy, contrast-enhanced CT imaging, and T2-weighted magnetic resonance imaging, alongside evaluating its exceptional biocompatibility at both cellular and in vivo levels using a mouse breast tumor allograft model. Notably, the tantalum component of Ta_4C_3-IONP-SPs demonstrated remarkable performance in contrast-enhanced CT imaging owing to its high

atomic number and X-ray attenuation coefficient, while the integrated superparamagnetic IONPs served as outstanding contrast agents for T2-weighted magnetic resonance imaging. The Ta_4C_3-IONP-SPs composite nanosheets, with their exceptional photothermal conversion efficiency, achieved complete eradication of tumors without recurrence, underscoring their remarkable efficacy in breast tumor photo-ablation (Z. Liu, Lin, et al., 2018).

Hua et al. did a research where they created a successful photothermal therapy method for antibacterial, anti-inflammatory, and wound healing purposes utilizing $Mo_2Ti_2C_3$. Their results showed that $Mo_2Ti_2C_3$ had increased bacteria-killing ability when exposed to NIR light. Research on rats shown that bacterial keratitis inhibited MRSA infection in the rats. The inflammatory response has been shown to be inhibited gradually (Hua, Huang, Le, & Huang, 2023). As shown in Table 2.2, studies in which immunotherapy is used in combination with PDT/PTT studies with Mxenes are very limited. In fact, when we look at the literature, there is no cancer study in which PTT and immunotherapy using $Mo_2Ti_2C_3$ are used in combination.

6. CONCLUSION

In this thesis, the photothermal and photodynamic effects of different MXenes on 4T1 cells under different wavelengths of light were investigated, as well as whether the material supports immunotherapy after PTT&PDT. Cell viability experiments were performed using $Mo_2Ti_2C_3$, Nb_4C_3 and Ta_4C_3 MXenes at different wavelengths and different concentrations. It was determined that the viability of 4T1 breast cancer cells treated with $Mo_2Ti_2C_3$ material decreased by 90% after PTT. The exposure time of the $Mo_2Ti_2C_3$ material tested at a dose of 200 µg / ml to 850 nm wavelength LED light was tested in half an hour, one hour and 2 hours periods and the use of 1 hour light exposure time was preferred in terms of cell viability. According to the results of the research, it was determined that $Mo_2Ti_2C_3$ material showed photothermal effect at 850 nm wavelength in temperature measurement experiments. At the same time, as expected in the experimental results for the examination of ROS activity, ROS release was not detected in 4T1 breast cancer cells treated with $Mo_2Ti_2C_3$ and exposed to 850 nm wavelength light for 1 hour. In line with these results, it is possible to say that the treatment is PTT. With this research, promising results were obtained for the first time in the literature by using $Mo_2Ti_2C_3$ as a photosensitiser in PTT.

TEM analyses were performed to examine the triggering of ICD, which is a result of immunotherapy in the presence of PTT, which is another unique feature of the thesis. In accordance with the TEM analyses, it was determined that 4T1 cells took up the material after PTT and CAL1 cells took up the material after the PTT protocol. Considering the differences between the groups as a result of the examination, it can be observed that immunotherapy is triggered after PTT with $Mo_2Ti_2C_3$ material.

In conclusion, in the light of the data obtained in this thesis study, $Mo_2Ti_2C_3$ material, which has not been used for cancer treatment in the literature before, has been used as photosensitiser nanoparticles and it is predicted that the combined use of PTT and Immunotherapy for breast cancer treatment will contribute to cancer studies in the literature.

REFERENCES

Adjei, I. M., & Blanka, S. (2015). Modulation of the tumor microenvironment for cancer treatment: a biomaterials approach. *Journal of functional biomaterials, 6*(1), 81-103.

Aggarwal, S. (2010). Targeted cancer therapies. *Nature reviews. Drug discovery, 9*(6), 427.

Aghajanzadeh, M., Zamani, M., Rajabi Kouchi, F., Eixenberger, J., Shirini, D., Estrada, D., & Shirini, F. (2022). Synergic antitumor effect of photodynamic therapy and chemotherapy mediated by nano drug delivery systems. *Pharmaceutics, 14*(2), 322.

Ahmad, R., Fu, J., He, N., & Li, S. (2016). Advanced gold nanomaterials for photothermal therapy of cancer. *Journal of nanoscience and nanotechnology, 16*(1), 67-80.

Akhavan, O., & Ghaderi, E. (2013). Graphene nanomesh promises extremely efficient in vivo photothermal therapy. *Small, 9*(21), 3593-3601.

Akhavan, O., Ghaderi, E., Aghayee, S., Fereydooni, Y., & Talebi, A. (2012). The use of a glucose-reduced graphene oxide suspension for photothermal cancer therapy. *Journal of Materials Chemistry, 22*(27), 13773-13781.

Bailey, K. M., Wojtkowiak, J. W., Hashim, A. I., & Gillies, R. J. (2012). Targeting the metabolic microenvironment of tumors. *Advances in pharmacology, 65*, 63-107.

Ban, Q., Bai, T., Duan, X., & Kong, J. (2017). Noninvasive photothermal cancer therapy nanoplatforms via integrating nanomaterials and functional polymers. *Biomaterials science, 5*(2), 190-210.

Baskar, R., Lee, K. A., Yeo, R., & Yeoh, K.-W. (2012). Cancer and radiation therapy: current advances and future directions. *International journal of medical sciences, 9*(3), 193.

Begg, A. C., Stewart, F. A., & Vens, C. (2011). Strategies to improve radiotherapy with targeted drugs. *Nature reviews cancer, 11*(4), 239-253.

Bhole, R., Bonde, C., Kadam, P., & Wavwale, R. (2021). A comprehensive review on photodynamic therapy (PDT) and photothermal therapy (PTT) for cancer treatment. *Turkish Journal of Oncology, 36*(1).

Brown, S. B., Brown, E. A., & Walker, I. (2004). The present and future role of photodynamic therapy in cancer treatment. *The lancet oncology, 5*(8), 497-508.

Cairns, J. (1985). The treatment of diseases and the war against cancer. *Scientific American, 253*(5), 51-59.

Carr, C., Ng, J., & Wigmore, T. (2008). The side effects of chemotherapeutic agents. *Current Anaesthesia & Critical Care, 19*(2), 70-79.

Chang, J. C. (2016). Cancer stem cells: Role in tumor growth, recurrence, metastasis, and treatment resistance. *Medicine, 95*(Suppl 1).

Chen, J., Fan, T., Xie, Z., Zeng, Q., Xue, P., Zheng, T., . . . Zhang, H. (2020). Advances in nanomaterials for photodynamic therapy applications: Status and challenges. *Biomaterials, 237*, 119827.

Chen, Q., Xu, L., Liang, C., Wang, C., Peng, R., & Liu, Z. (2016). Photothermal therapy with immune-adjuvant nanoparticles together with checkpoint blockade for effective cancer immunotherapy. *Nature communications, 7*(1), 13193.

Chen, Y., Wang, L., & Shi, J. (2016). Two-dimensional non-carbonaceous materials-enabled efficient photothermal cancer therapy. *Nano today, 11*(3), 292-308.

Chen, Y., Wu, Y., Sun, B., Liu, S., & Liu, H. (2017). Two-dimensional nanomaterials for cancer nanotheranostics. *Small, 13*(10), 1603446.

Cheng, L., Wang, C., Feng, L., Yang, K., & Liu, Z. (2014). Functional nanomaterials for phototherapies of cancer. *Chemical reviews, 114*(21), 10869-10939.

Cheng, L., Wang, X., Gong, F., Liu, T., & Liu, Z. (2020). 2D nanomaterials for cancer theranostic applications. *Advanced Materials, 32*(13), 1902333.

Chidambaram, M., Manavalan, R., & Kathiresan, K. (2011). Nanotherapeutics to overcome conventional cancer chemotherapy limitations. *Journal of pharmacy & pharmaceutical sciences, 14*(1), 67-77.

Chu, D.-T., Nguyen, T. T., Tien, N. L. B., Tran, D.-K., Jeong, J.-H., Anh, P. G., . . . Dinh, T. C. (2020). Recent progress of stem cell therapy in cancer treatment: molecular mechanisms and potential applications. *Cells, 9*(3), 563.

Citri, A., & Yarden, Y. (2006). EGF–ERBB signalling: towards the systems level. *Nature reviews Molecular cell biology, 7*(7), 505-516.

Dai, C., Chen, Y., Jing, X., Xiang, L., Yang, D., Lin, H., . . . Wu, R. (2017). Two-dimensional tantalum carbide (MXenes) composite nanosheets for multiple imaging-guided photothermal tumor ablation. *Acs Nano, 11*(12), 12696-12712.

Dai, C., Lin, H., Xu, G., Liu, Z., Wu, R., & Chen, Y. (2017). Biocompatible 2D titanium carbide (MXenes) composite nanosheets for pH-responsive MRI-guided tumor hyperthermia. *Chemistry of Materials, 29*(20), 8637-8652.

Daniell, M., & Hill, J. (1991). A history of photodynamic therapy. *Australian and New Zealand Journal of Surgery, 61*(5), 340-348.

Das, M., Mohanty, C., & Sahoo, S. K. (2009). Ligand-based targeted therapy for cancer tissue. *Expert opinion on drug delivery, 6*(3), 285-304.

Debele, T. A., Peng, S., & Tsai, H.-C. (2015). Drug carrier for photodynamic cancer therapy. *International journal of molecular sciences, 16*(9), 22094-22136.

Dillman, R. O. (2011). Cancer immunotherapy. *Cancer biotherapy & radiopharmaceuticals, 26*(1), 1-64.

Dolmans, D. E., Fukumura, D., & Jain, R. K. (2003). Photodynamic therapy for cancer. *Nature reviews cancer, 3*(5), 380-387.

Doughty, A. C., Hoover, A. R., Layton, E., Murray, C. K., Howard, E. W., & Chen, W. R. (2019). Nanomaterial applications in photothermal therapy for cancer. *Materials, 12*(5), 779.

Dulbecco, R. (1986). A turning point in cancer research: sequencing the human genome. *science, 231*(4742), 1055-1056.

Erkekoğlu, P., & BAYDAR, T. (2021). Güncel in vitro sitotoksisite testleri. *Hacettepe University Journal of the Faculty of Pharmacy, 41*(1), 45-63.

Eruslanov, E., & Kusmartsev, S. (2010). Identification of ROS using oxidized DCFDA and flow-cytometry. *Advanced protocols in oxidative stress II*, 57-72.

Eskiizmir, G., Baskın, Y., & Yapıcı, K. (2018). Graphene-based nanomaterials in cancer treatment and diagnosis. In *Fullerens, graphenes and nanotubes* (pp. 331-374): Elsevier.

Finsen, N. R. (1901). *Phototherapy: 1. The Chemical Rays of Light and Smallpox, 2. Light as a Stimulant, 3. The Treatment of Lupus Vulgarisby Concentrated Chemical Rays*: Arnold.

Fisher, B., Brown, A., Mamounas, E., Wieand, S., Robidoux, A., Margolese, R. G., . . . Wolmark, N. (1997). Effect of preoperative chemotherapy on local-regional disease in women with operable breast cancer: findings from National Surgical Adjuvant Breast and Bowel Project B-18. *Journal of clinical oncology, 15*(7), 2483-2493.

Fotakis, G., & Timbrell, J. A. (2006). In vitro cytotoxicity assays: comparison of LDH, neutral red, MTT and protein assay in hepatoma cell lines following exposure to cadmium chloride. *Toxicology letters, 160*(2), 171-177.

Frederick, L., Page, D. L., Fleming, I. D., Fritz, A. G., Balch, C. M., Haller, D. G., & Morrow, M. (2002). *AJCC cancer staging manual*: Springer Science & Business Media.

Gasson, J. C. (1991). Molecular physiology of granulocyte-macrophage colony-stimulating factor.

Gilman, A. (1963). The initial clinical trial of nitrogen mustard. *The American Journal of Surgery, 105*(5), 574-578.

Gomer, C., Ferrario, A., & Fisher, A. (2001). Photodynamic therapy: basic mechanisms and molecular applications. *Photobiology for the 21st century. Overland Park Kansas: Valdenmar Publishing Company*, 143-147.

Greenberg, P., Hortobagyi, G. N., Smith, T. L., Ziegler, L. D., Frye, D. K., & Buzdar, A. U. (1996). Long-term follow-up of patients with complete remission following combination chemotherapy for metastatic breast cancer. *Journal of clinical oncology, 14*(8), 2197-2205.

Halim, J., Kota, S., Lukatskaya, M. R., Naguib, M., Zhao, M. Q., Moon, E. J., . . . Gogotsi, Y. (2016). Synthesis and characterization of 2D molybdenum carbide (MXene). *Advanced Functional Materials, 26*(18), 3118-3127.

Halsted, W. S. (1894). I. The results of operations for the cure of cancer of the breast performed at the Johns Hopkins Hospital from June, 1889, to January, 1894. *Annals of surgery, 20*(5), 497.

Hamilton, J. A. (2008). Colony-stimulating factors in inflammation and autoimmunity. *Nature Reviews Immunology, 8*(7), 533-544.

Han, Q., Wang, X., Jia, X., Cai, S., Liang, W., Qin, Y., . . . Wang, C. (2017). CpG loaded MoS 2 nanosheets as multifunctional agents for photothermal enhanced cancer immunotherapy. *Nanoscale, 9*(18), 5927-5934.

Han, X., Huang, J., Lin, H., Wang, Z., Li, P., & Chen, Y. (2018). 2D ultrathin MXene-based drug-delivery nanoplatform for synergistic photothermal ablation and chemotherapy of cancer. *Advanced healthcare materials, 7*(9), 1701394.

Han, X., Jing, X., Yang, D., Lin, H., Wang, Z., Ran, H., . . . Chen, Y. (2018). Therapeutic mesopore construction on 2D Nb2C MXenes for targeted and enhanced chemo-photothermal cancer therapy in NIR-II biowindow. *Theranostics, 8*(16), 4491.

Health, N. I. o. (1991). *Treatment of early stage breast cancer.* Paper presented at the NIH Consensus Development Conference.

Henderson, B. W., & Dougherty, T. J. (1992). How does photodynamic therapy work? *Photochemistry and photobiology, 55*(1), 145-157.

Hinrichs, C. S., Stevanovic, S., Draper, L., Somerville, R., Wunderlich, J., Restifo, N. P., . . . Yang, J. C. (2014). HPV-targeted tumor-infiltrating lymphocytes for cervical cancer. In: American Society of Clinical Oncology.

Hirsch, L. R., Stafford, R. J., Bankson, J., Sershen, S. R., Rivera, B., Price, R., . . . West, J. L. (2003). Nanoshell-mediated near-infrared thermal therapy of tumors under magnetic resonance guidance. *Proceedings of the National Academy of Sciences, 100*(23), 13549-13554.

Hortobagyi, G. N. (1998). Treatment of breast cancer. *New England Journal of Medicine, 339*(14), 974-984.

Hortobagyi, G. N., & Buzdar, A. U. (1995). Current status of adjuvant systemic therapy for primary breast cancer: progress and controversy. *CA: A Cancer Journal for Clinicians, 45*(4), 199-226.

Hortobagyi, G. N., & Piccart-Gebhart, M. J. (1996). *Current management of advanced breast cancer.* Paper presented at the Seminars in Oncology.

Hsiao, C.-W., Chuang, E.-Y., Chen, H.-L., Wan, D., Korupalli, C., Liao, Z.-X., . . . Sung, H.-W. (2015). Photothermal tumor ablation in mice with repeated therapy sessions using NIR-absorbing micellar hydrogels formed in situ. *Biomaterials, 56*, 26-35.

Hua, S., Huang, B., Le, Z., & Huang, Q. (2023). Mo-based Mo2Ti2C3 MXene as photothermal nanoagents to eradicating methicillin-resistant Staphylococcus aureus with photothermal therapy. *Materials & Design, 231*, 112033.

Huang, X., Lu, Y., Guo, M., Du, S., & Han, N. (2021). Recent strategies for nano-based PTT combined with immunotherapy: from a biomaterial point of view. *Theranostics, 11*(15), 7546.

Hwang, S., Nam, J., Jung, S., Song, J., Doh, H., & Kim, S. (2014). Gold nanoparticle-mediated photothermal therapy: current status and future perspective. *Nanomedicine, 9*(13), 2003-2022.

Jackson, S. P., & Bartek, J. (2009). The DNA-damage response in human biology and disease. *Nature, 461*(7267), 1071-1078.

Khalil, C., Moussa, M., Azar, A., Tawk, J., Habbouche, J., Salameh, R., . . . Alaaeddine, N. (2019). Anti-proliferative effects of mesenchymal stem cells (MSCs) derived from multiple sources on ovarian cancer cell lines: an in-vitro experimental study. *Journal of Ovarian Research, 12*(1), 1-12.

Kirkwood, J. M., Tarhini, A. A., Panelli, M. C., Moschos, S. J., Zarour, H. M., Butterfield, L. H., & Gogas, H. J. (2008). Next generation of immunotherapy for melanoma. *Journal of clinical oncology, 26*(20), 3445-3455.

Konopleva, M., Pollyea, D. A., Potluri, J., Chyla, B., Hogdal, L., Busman, T., . . . Ricker, J. L. (2016). Efficacy and biological correlates of response in a phase II study of venetoclax monotherapy in patients with acute myelogenous leukemia. *Cancer discovery, 6*(10), 1106-1117.

Korupalli, C., You, K.-L., Getachew, G., Rasal, A. S., Direrso, W. B., Zakki Fahmi, M., & Chang, J.-Y. (2022). Engineering the surface of Ti3C2 MXene nanosheets for high stability and multimodal anticancer therapy. *Pharmaceutics, 14*(2), 304.

Kyrylenko, S., Gogotsi, O., Baginskiy, I., Balitskyi, V., Zahorodna, V., Husak, Y., . . . Lyndin, M. (2022). Mxene-assisted ablation of cells with a pulsed near-infrared laser. *ACS applied materials & interfaces, 14*(25), 28683-28696.

Lander, E., Linton, L., & Birren, B. (2001). Initial sequencing and analysis of the human genome [published correction appears in Nature. 2001; 411 (6838): 720]. *Nature, 409*(6822), 860-921.

Li, J., Cai, X., Zhang, Y., Li, K., Guan, L., Li, Y., . . . Sun, T. (2022). MnO2 Nanozyme-Loaded MXene for Cancer Synergistic Photothermal-Chemodynamic Therapy. *ChemistrySelect, 7*(23), e202201127.

Li, Z., Zhang, H., Han, J., Chen, Y., Lin, H., & Yang, T. (2018). Surface nanopore engineering of 2D MXenes for targeted and synergistic multitherapies of hepatocellular carcinoma. *Advanced Materials, 30*(25), 1706981.

Liao, L., Bai, J., Cheng, R., Lin, Y.-C., Jiang, S., Huang, Y., & Duan, X. (2010). Top-gated graphene nanoribbon transistors with ultrathin high-k dielectrics. *Nano letters, 10*(5), 1917-1921.

Lin, H., Gao, S., Dai, C., Chen, Y., & Shi, J. (2017). A two-dimensional biodegradable niobium carbide (MXene) for photothermal tumor eradication in NIR-I and NIR-II biowindows. *Journal of the American Chemical Society, 139*(45), 16235-16247.

Lin, H., Wang, X., Yu, L., Chen, Y., & Shi, J. (2017). Two-dimensional ultrathin MXene ceramic nanosheets for photothermal conversion. *Nano letters, 17*(1), 384-391.

Lin, H., Wang, Y., Gao, S., Chen, Y., & Shi, J. (2018). Theranostic 2D tantalum carbide (MXene). *Advanced Materials, 30*(4), 1703284.

Lin, Y., Xu, S., Zhao, X., Chang, L., Hu, Y., Chen, Z., . . . Chen, D. (2022). Preparation of NIR-sensitive, photothermal and photodynamic multi-functional Mxene nanosheets for laryngeal cancer therapy by regulating mitochondrial apoptosis. *Materials & Design*, 110887.

Liu, A., Liu, Y., Liu, G., Zhang, A., Cheng, Y., Li, Y., . . . Liu, J. (2022). Engineering of surface modified Ti3C2Tx MXene based dually controlled drug release system for synergistic multitherapies of cancer. *Chemical Engineering Journal, 448*, 137691.

Liu, G., Zou, J., Tang, Q., Yang, X., Zhang, Y., Zhang, Q., . . . Dong, X. (2017). Surface modified Ti3C2 MXene nanosheets for tumor targeting photothermal/photodynamic/chemo synergistic therapy. *ACS applied materials & interfaces, 9*(46), 40077-40086.

Liu, J.-n., Bu, W., & Shi, J. (2017). Chemical design and synthesis of functionalized probes for imaging and treating tumor hypoxia. *Chemical reviews, 117*(9), 6160-6224.

Liu, K., Liao, Y., Zhou, Z., Zhang, L., Jiang, Y., Lu, H., . . . Li, Z. (2022). Photothermal-triggered immunogenic nanotherapeutics for optimizing osteosarcoma therapy by synergizing innate and adaptive immunity. *Biomaterials, 282*, 121383.

Liu, Y., Han, Q., Yang, W., Gan, X., Yang, Y., Xie, K., . . . Deng, Y. (2020). Two-dimensional MXene/cobalt nanowire heterojunction for controlled drug delivery and chemo-photothermal therapy. *Materials Science and Engineering: C, 116*, 111212.

Liu, Z., Lin, H., Zhao, M., Dai, C., Zhang, S., Peng, W., & Chen, Y. (2018). 2D superparamagnetic tantalum carbide composite MXenes for efficient breast-cancer theranostics. *Theranostics, 8*(6), 1648.

Liu, Z., Zhao, M., Lin, H., Dai, C., Ren, C., Zhang, S., . . . Chen, Y. (2018). 2D magnetic titanium carbide MXene for cancer theranostics. *Journal of Materials Chemistry B, 6*(21), 3541-3548.

Lordick, F., & Gockel, I. (2016). Chances, risks and limitations of neoadjuvant therapy in surgical oncology. *Innovative Surgical Sciences, 1*(1), 3-11.

Lu, B., Zhu, Z., Ma, B., Wang, W., Zhu, R., & Zhang, J. (2021). 2D MXene nanomaterials for versatile biomedical applications: current trends and future prospects. *Small, 17*(46), 2100946.

Luo, L., Shu, R., & Wu, A. (2017). Nanomaterial-based cancer immunotherapy. *Journal of Materials Chemistry B, 5*(28), 5517-5531.

Ma, H., Jiang, C., Zhai, D., Luo, Y., Chen, Y., Lv, F., . . . Chang, J. (2016). A bifunctional biomaterial with photothermal effect for tumor therapy and bone regeneration. *Advanced Functional Materials, 26*(8), 1197-1208.

Metcalf, D. (1985). The granulocyte-macrophage colony-stimulating factors. *science, 229*(4708), 16-22.

Misra, R., Acharya, S., & Sahoo, S. K. (2010). Cancer nanotechnology: application of nanotechnology in cancer therapy. *Drug discovery today, 15*(19-20), 842-850.

Naguib, M., Kurtoglu, M., Presser, V., Lu, J., Niu, J., Heon, M., . . . Barsoum, M. W. (2011). Two-dimensional nanocrystals produced by exfoliation of Ti3AlC2. *Advanced Materials, 23*(37), 4248-4253.

Naguib, M., Mochalin, V. N., Barsoum, M. W., & Gogotsi, Y. (2014). 25th anniversary article: MXenes: a new family of two-dimensional materials. *Advanced Materials, 26*(7), 992-1005.

Nunes, S. S., Miranda, S. E. M., de Oliveira Silva, J., Fernandes, R. S., de Alcântara Lemos, J., de Aguiar Ferreira, C., . . . de Barros, A. L. B. (2021). pH-responsive and folate-coated liposomes encapsulating irinotecan as an alternative to improve efficacy of colorectal cancer treatment. *Biomedicine & Pharmacotherapy, 144*, 112317.

Oleinick, N. L., Morris, R. L., & Belichenko, I. (2002). The role of apoptosis in response to photodynamic therapy: what, where, why, and how. *Photochemical & Photobiological Sciences, 1*(1), 1-21.

Oncology, A. S. o. C. (1997). Recommended breast cancer surveillance guidelines. *J Clin Oncol, 15*, 2149-2156.

Ouyang, X., Telli, M. L., & Wu, J. C. (2019). Induced pluripotent stem cell-based cancer vaccines. *Frontiers in Immunology, 10*, 1510.

Palucka, K., & Banchereau, J. (2012). Cancer immunotherapy via dendritic cells. *Nature reviews cancer, 12*(4), 265-277.

Pan, J., Wang, Y., Zhang, C., Wang, X., Wang, H., Wang, J., . . . Yu, C. (2018). Antigen-directed fabrication of a multifunctional nanovaccine with ultrahigh antigen loading efficiency for tumor photothermal-immunotherapy. *Advanced Materials, 30*(8), 1704408.

Pan, J., Zhang, M., Fu, G., Zhang, L., Yu, H., Yan, X., . . . Liu, X. (2022). Ti3C2 MXene Nanosheets Functionalized with NaErF4: 0.5% Tm@ NaLuF4 Nanoparticles for Dual-Modal Near-Infrared IIb/Magnetic Resonance Imaging-Guided Tumor Hyperthermia. *ACS Applied Nano Materials*.

Paulis, L. E., Mandal, S., Kreutz, M., & Figdor, C. G. (2013). Dendritic cell-based nanovaccines for cancer immunotherapy. *Current opinion in immunology, 25*(3), 389-395.

Peeters, F., Verbeeten Jr, B., & Venema, H. (1979). Nobel Prize for medicine and physiology 1979 for AM Cormack and GN Hounsfield. *Nederlands tijdschrift voor geneeskunde, 123*(51), 2192-2193.

Pegram, M. D., Konecny, G., & Slamon, D. J. (2000). The molecular and cellular biology of HER2/neu gene amplification/overexpression and the clinical development of herceptin (trastuzumab) therapy for breast cancer. *Advances in Breast Cancer Management*, 57-75.

Reddy, R. L. (2005). Mobilization and collection of peripheral blood progenitor cells for transplantation. *Transfusion and Apheresis Science, 32*(1), 63-72.

Reichert, J. M., & Wenger, J. B. (2008). Development trends for new cancer therapeutics and vaccines. *Drug discovery today, 13*(1-2), 30-37.

Richie, R. C., & Swanson, J. O. (2003). Breast cancer: a review of the literature. *JOURNAL OF INSURANCE MEDICINE-NEW YORK THEN DENVER--, 35*(2), 85-101.

Robinson, J. T., Tabakman, S. M., Liang, Y., Wang, H., Sanchez Casalongue, H., Vinh, D., & Dai, H. (2011). Ultrasmall reduced graphene oxide with high near-infrared absorbance for photothermal therapy. *Journal of the American Chemical Society, 133*(17), 6825-6831.

Roy, A., & Li, S. D. (2016). Modifying the tumor microenvironment using nanoparticle therapeutics. *Wiley Interdisciplinary Reviews: nanomedicine and nanobiotechnology, 8*(6), 891-908.

Shao, J., Zhang, J., Jiang, C., Lin, J., & Huang, P. (2020). Biodegradable titanium nitride MXene quantum dots for cancer phototheranostics in NIR-I/II biowindows. *Chemical Engineering Journal, 400*, 126009.

Singhal, S., Nie, S., & Wang, M. D. (2010). Nanotechnology applications in surgical oncology. *Annual review of medicine, 61*, 359-373.

Sobolčiak, P., Tanvir, A., Sadasivuni, K. K., & Krupa, I. (2019). Piezoresistive sensors based on electrospun mats modified by 2D Ti3C2Tx MXene. *Sensors, 19*(20), 4589.

Soleymaniha, M., Shahbazi, M. A., Rafieerad, A. R., Maleki, A., & Amiri, A. (2019). Promoting role of MXene nanosheets in biomedical sciences: therapeutic and biosensing innovations. *Advanced healthcare materials, 8*(1), 1801137.

Sourati, A., Ameri, A., & Malekzadeh, M. (2017). Acute side effects of radiation therapy. *Cham: Springer*.

Spikes, J. (1985). Primary photoprocesses in biology and medicine. *Berghausen, RV, Jori, G., Land, EJ, Truscott, TH, Eds*, 209-227.

Strachan, T., & Read, A. (1999). Gene therapy and other molecular genetic-based therapeutic approaches. *Human molecular genetics, 2*.

Stuart, N., Warwick, J., Blackledge, G., Spooner, D., Keen, C., Taylor, A., . . . Earl, H. (1996). A randomised phase III cross-over study of tamoxifen versus megestrol acetate in advanced and recurrent breast cancer. *European Journal of Cancer, 32*(11), 1888-1892.

Sung, H., Ferlay, J., Siegel, R. L., Laversanne, M., Soerjomataram, I., Jemal, A., & Bray, F. (2021). Global cancer statistics 2020: GLOBOCAN estimates of incidence and mortality worldwide for 36 cancers in 185 countries. *CA: A Cancer Journal for Clinicians, 71*(3), 209-249.

Sweeney, E. E., Cano-Mejia, J., & Fernandes, R. (2018). Photothermal therapy generates a thermal window of immunogenic cell death in neuroblastoma. *Small, 14*(20), 1800678.

Szuplewska, A., Kulpińska, D., Dybko, A., Jastrzębska, A. M., Wojciechowski, T., Rozmysłowska, A., . . . Brzózka, Z. (2019). 2D Ti2C (MXene) as a novel highly efficient and selective agent for photothermal therapy. *Materials Science and Engineering: C, 98*, 874-886.

Tang, C., & Yang, Z. (2017). Transmission electron microscopy (TEM). In *Membrane characterization* (pp. 145-159): Elsevier.

Tang, W., Dong, Z., Zhang, R., Yi, X., Yang, K., Jin, M., . . . Cheng, L. (2018). Multifunctional two-dimensional core–shell mxene@ gold nanocomposites for enhanced photo–radio combined therapy in the second biological window. *ACS nano, 13*(1), 284-294.

Tao, Y., Ju, E., Ren, J., & Qu, X. (2014). Immunostimulatory oligonucleotides-loaded cationic graphene oxide with photothermally enhanced immunogenicity for photothermal/immune cancer therapy. *Biomaterials, 35*(37), 9963-9971.

Thariat, J., Hannoun-Levi, J.-M., Sun Myint, A., Vuong, T., & Gérard, J.-P. (2013). Past, present, and future of radiotherapy for the benefit of patients. *Nature reviews Clinical oncology, 10*(1), 52-60.

Thor, A. (2004). A revised staging system for breast cancer. *The breast journal, 10*, S15-S18.

Vakhshiteh, F., Atyabi, F., & Ostad, S. N. (2019). Mesenchymal stem cell exosomes: a two-edged sword in cancer therapy. *International journal of nanomedicine*, 2847-2859.

Valter, K., Chen, L., Kruspig, B., Maximchik, P., Cui, H., Zhivotovsky, B., & Gogvadze, V. (2017). Contrasting effects of glutamine deprivation on apoptosis induced by conventionally used anticancer drugs. *Biochimica et Biophysica Acta (BBA)-Molecular Cell Research, 1864*(3), 498-506.

Venter, J. C., Adams, M. D., Myers, E. W., Li, P. W., Mural, R. J., Sutton, G. G., . . . Holt, R. A. (2001). The sequence of the human genome. *science, 291*(5507), 1304-1351.

Wang, X., & Cheng, L. (2019). Multifunctional two-dimensional nanocomposites for photothermal-based combined cancer therapy. *Nanoscale, 11*(34), 15685-15708.

Wang, Y., Niu, N., Huang, Y., Song, S., Tan, H., Wang, L., . . . Tang, B. Z. (2022). Three-Pronged Attack by Hybrid Nanoplatform Involving MXenes, Upconversion Nanoparticle and Aggregation-Induced Emission Photosensitizer for Potent Cancer Theranostics. *Small Methods*, 2200393.

Weichselbaum, R. R., & Kufe, D. (1997). Gene therapy of cancer. *The Lancet, 349*, S10-S12.

Wu, Y., Xiong, W., Wang, Z., Wang, Y., Sun, K.-y., Song, X., . . . Zou, X. (2022). Self-assembled MXene-based Schottky-junction upon Transition metal oxide for regulated tumor microenvironment and enhanced CDT/PTT/MRI activated by NIR irradiation. *Chemical Engineering Journal, 427*, 131925.

Xing, C., Chen, S., Liang, X., Liu, Q., Qu, M., Zou, Q., . . . Fan, D. (2018). Two-dimensional MXene (Ti3C2)-integrated cellulose hydrogels: toward smart three-dimensional network nanoplatforms exhibiting light-induced swelling and bimodal photothermal/chemotherapy anticancer activity. *ACS applied materials & interfaces, 10*(33), 27631-27643.

Xu, D., Yang, F., Qu, D., Wang, Z., Gu, L., Wu, W., & Lv, R. (2020). Transferred photothermal to photodynamic therapy based on the marriage of ultrathin titanium carbide and up-conversion nanoparticles. *Langmuir, 36*(43), 13060-13069.

Xu, Y., Wang, Y., An, J., Sedgwick, A. C., Li, M., Xie, J., . . . Steinbrueck, A. (2022). 2D-ultrathin MXene/DOXjade platform for iron chelation chemo-photothermal therapy. *Bioactive materials, 14*, 76-85.

Xu, Z., Ramishetti, S., Tseng, Y.-C., Guo, S., Wang, Y., & Huang, L. (2013). Multifunctional nanoparticles co-delivering Trp2 peptide and CpG adjuvant induce potent cytotoxic T-lymphocyte response against melanoma and its lung metastasis. *Journal of Controlled Release, 172*(1), 259-265.

Xuan, J., Wang, Z., Chen, Y., Liang, D., Cheng, L., Yang, X., . . . Geng, F. (2016). Organic-base-driven intercalation and delamination for the production of functionalized titanium carbide nanosheets with superior photothermal therapeutic performance. *Angewandte Chemie, 128*(47), 14789-14794.

Yadav, P. (2017). Targeted cancer therapy; researchers reflection. *Int Peer-Rev J, 1*, 11-17.

You, Q., Peng, J., Chang, Z., Ge, M., Mei, Q., & Dong, W.-F. (2021). Specific recognition and photothermal release of circulating tumor cells using near-infrared light-responsive 2D MXene nanosheets@ hydrogel membranes. *Talanta, 235*, 122770.

Yu, X., Cai, X., Cui, H., Lee, S.-W., Yu, X.-F., & Liu, B. (2017). Fluorine-free preparation of titanium carbide MXene quantum dots with high near-infrared photothermal performances for cancer therapy. *Nanoscale, 9*(45), 17859-17864.

Zhang, C., Bu, W., Ni, D., Zuo, C., Cheng, C., Li, Q., . . . Shi, J. (2016). A polyoxometalate cluster paradigm with self-adaptive electronic structure for acidity/reducibility-specific photothermal conversion. *Journal of the American Chemical Society, 138*(26), 8156-8164.

Zhang, D.-Y., Liu, H., Younis, M. R., Lei, S., Chen, Y., Huang, P., & Lin, J. (2022). In-situ TiO2-x decoration of titanium carbide MXene for photo/sono-responsive antitumor theranostics. *Journal of Nanobiotechnology, 20*(1), 1-14.

Zhang, Q., Huang, W., Yang, C., Wang, F., Song, C., Gao, Y., . . . Guo, C. (2019). The theranostic nanoagent Mo 2 C for multi-modal imaging-guided cancer synergistic phototherapy. *Biomaterials science, 7*(7), 2729-2739.

Zhang, X., Cheng, L., Lu, Y., Tang, J., Lv, Q., Chen, X., . . . Liu, J. (2022). A mxene-based bionic cascaded-enzyme nanoreactor for tumor phototherapy/enzyme dynamic therapy and hypoxia-activated chemotherapy. *Nano-Micro Letters, 14*(1), 1-21.

Zhang, Z.-J., Wang, K.-P., Mo, J.-G., Xiong, L., & Wen, Y. (2020). Photodynamic therapy regulates fate of cancer stem cells through reactive oxygen species. *World Journal of Stem Cells, 12*(7), 562.

Zhou, B., Yin, H., Dong, C., Sun, L., Feng, W., Pu, Y., . . . Xu, H. (2021). Biodegradable and Excretable 2D W1. 33C i-MXene with Vacancy Ordering for Theory-Oriented Cancer Nanotheranostics in Near-Infrared Biowindow. *Advanced Science, 8*(24), 2101043.

Zhou, Z., Li, X., Hu, T., Xue, B., Chen, H., Ma, L., . . . Tan, C. (2022). Molybdenum-Based Nanomaterials for Photothermal Cancer Therapy. *Advanced NanoBiomed Research, 2*(11), 2200065.

Zong, L., Wu, H., Lin, H., & Chen, Y. (2018a). A polyoxometalate-functionalized two-dimensional titanium carbide composite MXene for effective cancer theranostics. *Nano Research, 11*, 4149-4168.

Zong, L., Wu, H., Lin, H., & Chen, Y. (2018b). A polyoxometalate-functionalized two-dimensional titanium carbide composite MXene for effective cancer theranostics. *Nano Research, 11*(8), 4149-4168.

Zou, W. (2005). Immunosuppressive networks in the tumour environment and their therapeutic relevance. *Nature reviews cancer, 5*(4), 263-274.